NASA TECHNICAL NOTE

NASA TN D-3045
c. 1

NASA TN D-3045

INVESTIGATION OF A JET CONDENSER FOR SPACE POWER

by Robert J. Platt, Jr.

Langley Research Center

Langley Station, Hampton, Va.

NATIONAL AERONAUTICS AND SPACE ADMINISTRATION • WASHINGTON, D. C. • OCTOBER 1965

NASA TN D-3045

INVESTIGATION OF A JET CONDENSER FOR SPACE POWER

By Robert J. Platt, Jr.

Langley Research Center
Langley Station, Hampton, Va.

NATIONAL AERONAUTICS AND SPACE ADMINISTRATION

For sale by the Clearinghouse for Federal Scientific and Technical Information
Springfield, Virginia 22151 – Price $2.00

INVESTIGATION OF A JET CONDENSER FOR SPACE POWER

By Robert J. Platt, Jr.
Langley Research Center

SUMMARY

An exploratory ground-based investigation has been made of a jet condenser of a type for which operation should be little affected by gravitational forces. Steam was condensed by water, the steam entering the condenser through a central nozzle and water entering through a surrounding annular nozzle. The steam and water flowed horizontally through a condenser tube, condensation of the steam occurring through direct contact with the water. The variables included water temperature and velocity, steam static pressure and velocity, and the ratio of steam nozzle area to water nozzle area. The water velocity entering the condenser was varied from 20 to 60 ft/sec (6.1 to 18.3 m/s); the entering steam velocity, from 600 to 1100 ft/sec (183 to 335 m/s); and entering steam static pressure, from 10 to 15 lbf/in^2 (69 to 103 kN/m^2).

The condensation length was affected by the flow variables and nozzle configuration. An empirical parameter was found which provided a rough correlation of the experimental condensation-length data.

Through the expenditure of pumping power, the jet condenser was able to increase the static pressure of the condensate by an amount several times the vapor dynamic pressure. A relatively large ratio of steam nozzle area to water nozzle area was found to be more efficient in that pressure augmentation was accomplished with less pumping power required per unit steam flow; however, a large nozzle area ratio increased the possibility that oscillations would develop in the flow. These oscillations could be avoided by operation at higher water inlet temperatures, which increased the condensation length, but which also increased the flow losses.

INTRODUCTION

Several electrical space-power systems in various stages of development are based on the Rankine cycle. This thermodynamic cycle requires that the working fluid, after leaving a turbine or other heat engine, be condensed from a vapor to a liquid and that the heat of condensation be rejected. In a space-power system the condenser must be able to operate under zero-gravity conditions, unlike condensers in industrial power plants which depend on gravity to separate the condensate from the vapor and to direct the condensate to a pump.

In most of the Rankine cycle space-power systems under consideration, the two operations of condensation and heat rejection are to be performed directly in a combined condenser-radiator. (For example, see ref. 1.) Such a direct condenser consists of finned tubes through which the vapor and condensate flow and which radiate the heat of condensation to space. Another type of condenser being considered for operation in space consists of a compact shell-and-tube heat exchanger, in which the vapor is condensed, and a separate liquid radiator. Still a third type of condenser is possible by eliminating the separating walls and allowing the vapor to mix with a cooler liquid of the same component. The resulting warmed liquid may then be cooled in a radiator, after which a part is returned to the boiler and the remainder is returned to the condenser inlet to continue the condensation process. This last condenser may be called a jet condenser and is a form of the industrial jet condenser modified to permit operation at zero-gravity conditions. It consists of a tube with vapor and liquid coolant introduced at one end and the resulting liquid mixture removed from the opposite end. The jet condenser appears advantageous because its operation should be little affected by gravitational forces, direct contact of vapor and coolant promises a high rate of heat transfer, and a large increase in static pressure from the vapor inlet to the condensate outlet is possible.

An investigation of jet condensers, in which mercury was the working fluid, has been reported in reference 1. Aside from its possible application to space-power systems, the jet condenser has also been proposed (ref. 2) as a means of condensing vapor to liquid in a space vehicle refrigeration system for cooling the contents of the space vehicle. References 1 and 2 are both concerned with a jet condenser in which the liquid coolant enters through a central nozzle and the vapor, through a surrounding annular nozzle. However, a jet condenser is also possible with the reverse arrangement; i.e., the vapor enters through the central nozzle and the liquid coolant, through the surrounding annular nozzle. The present report contains the results of a ground-based exploratory investigation of a jet condenser in which this latter physical arrangement, with water as the working fluid, is used. The variables included entering water temperature, entering water velocity from 20 to 60 ft/sec (6.1 to 18.3 m/s), and entering steam velocity from 600 to 1100 ft/sec (183 to 335 m/s). The jet condenser was tested with four different ratios of steam nozzle area to water nozzle area. Most of the data were obtained at an entering steam static pressure of 15 $\mathrm{lbf/in^2}$ (103 $\mathrm{kN/m^2}$); however, for one of the nozzle area ratios, data were obtained also at 10 $\mathrm{lbf/in^2}$ (69 $\mathrm{kN/m^2}$). (All values of pressure in this report are given as absolute rather than gage pressures.)

SYMBOLS

The units used for the physical quantities defined in this paper are given both in U.S. Customary Units and in the International System of Units (SI) (ref. 3). The appendix presents factors relating these two systems of units.

A	exit area of nozzle, ft^2 (m^2)
F	correlation factor, $\left(\frac{T_f - T_i}{T_{max} - T_i}\right)_l \left[\frac{v_l^{3/2}}{(V_v - V_l)^{1/2}}\right]_i \left(\frac{A_l}{A_v}\right)^{0.9} v_{i,v}$, $\frac{ft^4}{lbm\text{-}sec}$ $\left(\frac{m^4}{kg - s}\right)$
l	condensation length, in. (cm)
P	power, ft-lbf/sec (W)
p	static pressure, lbf/in^2 (kN/m^2)
p'	total pressure, lbf/in^2 (kN/m^2)
Q	condensation-heat-transfer rate, Btu/hr (W)
q	dynamic pressure, lbf/in^2 (N/m^2)
T	temperature, ^{o}F (^{o}K)
V	velocity, ft/sec (m/s)
v	specific volume, ft^3/lbm (m^3/kg)
$\frac{w_l}{w_v}$	ratio of liquid mass flow to vapor mass flow at entrance to condenser

Subscripts:

c	condensation
f	final (measured in diffuser)
i	initial (measured entering test section)
l	liquid
max	maximum
r	required
v	vapor

APPARATUS AND TEST METHODS

Test Loop

A schematic of the flow system used for the condenser tests is shown in figure 1. Water entered the test section through a nozzle, flowed through the test section, and entered a settling tank. From this tank the water passed through a centrifugal pump, a heat exchanger, and then returned to the test section. Steam was introduced into the test section through a central steam nozzle. The mixing of the steam and cooler water resulted in condensation of the steam and an increase in water temperature. The water temperature was reduced to its initial value by the heat exchanger to complete the cycle.

The initial water temperature was varied by changing the amount of cooling water flowing through the heat-exchanger shell and by adjusting the mixing valve. The water flow velocity was controlled by a globe valve following the mixing valve.

The static pressure of the flow system was regulated by varying the vapor pressure in the upper part of the settling tank. For tank pressures higher than atmospheric, steam was allowed to flow into the tank and escape to the atmosphere through a restricting valve. For tank pressures lower than atmospheric, a steam ejector was used to remove steam from the tank.

The steam supply line was provided with throttling valves, three steam separators connected in series, and a water line for adding moisture if needed. Throttling the steam supplied by a heating plant at 105 lbf/in^2 (724 kN/m^2) made it possible to obtain superheated steam at a lower pressure.

The stainless-steel nozzle assembly and method of attachment to the glass test section are shown in figure 2. The downstream end of the test section was attached to a stainless-steel diffuser section, of 10° total included angle, by a similar arrangement. The central nozzle, through which the steam entered the test section, was removable to permit the testing of several nozzle sizes. In addition to the 0.316-in. (0.803-cm) inside-diameter steam nozzle shown in figure 2, steam nozzles having inside diameters of 0.500 in. (1.270 cm), 0.418 in. (1.062 cm), and 0.158 in. (0.401 cm) were also tested. Substitution of one steam nozzle for another resulted also in a change in water-nozzle exit area, since the outer wall of the water nozzle was unchanged. The thickness of the steam-nozzle wall at the nozzle exit was 0.010 in. (0.025 cm) for all four nozzles.

The glass test section was about 30 in. (76 cm) long with walls 0.2 in. (0.5 cm) thick. The test section tapered linearly from a minimum inside diameter of 0.580 in. (1.473 cm) at the exit of the steam nozzle to 0.800 in. (2.032 cm) at the downstream end of the glass test section. The taper of the test section was provided to insure that the static pressure at the test-section wall would not decrease with distance downstream as a result of the thickening boundary layer.

A general view of the apparatus is given in figure 3. A clear plastic box is shown placed around the glass test section for protection in case of glass breakage.

Instrumentation

Temperatures and pressures within the nozzles, test section, and diffuser were measured with thermocouples and either static- or total-pressure tubes. The numerous thermometers and pressure gages shown in figure 3 were used only as aids in operating the test loop.

The manner of installation of the thermocouples and pressure tubes in the nozzle assembly and glass test section is shown in figure 2. The steam nozzle was instrumented with a static-pressure probe, extending along the nozzle axis, to measure the steam static pressure in the minimum-area (exit) section of the nozzle. In addition, the temperature and pressure at the entrance of the steam nozzle were measured by a thermocouple and a wall static-pressure tube.

The annular water nozzle was instrumented with four total-pressure tubes equally spaced around the annulus and all at the same axial location. These four tubes were connected to a manifold in order to provide a measurement of average water total pressure. A thermocouple was provided to measure the water temperature in the nozzle.

The glass test section was instrumented by drilling holes completely through the test-section walls and cementing thermocouples and static-pressure tubes in place. A thermocouple and a static-pressure tube were installed every 2 in. (5.1 cm) along the test section.

The diffuser following the glass test section was instrumented with a thermocouple and a total-pressure tube. The total-pressure tube was located at the center of the diffuser cross section, whose diameter was 2.85 in. (7.24 cm) at this station.

Thermocouple outputs were recorded directly as temperatures by multiple-point self-balancing potentiometers. The pressure tubes were connected to pressure transducers whose electrical outputs were recorded by other multiple-point self-balancing potentiometers.

Flow of the water entering the condenser was measured by a turbine flowmeter located in the line leading to the water nozzle. Two sizes of flowmeters were used to cover a wide range of water flow. The output of the flowmeter consisted of electrical pulses, which were measured by a frequency meter.

Tests

In preliminary testing, difficulty was experienced with air in the system and the resulting rusting of the carbon steel used for most of the test-loop components. It was believed that air was being sucked in around the pump shaft.

This flow was greatly reduced by connecting an elevated tank of water to the shaft stuffing box to provide a hydrostatic head on the shaft packing. During periods of nonoperation, such as overnight, the settling tank was connected to a low-pressure steam line to prevent the contamination of the system by air (see fig. 1). This arrangement provided pressurization of the system without overloading the pressure transducers.

As originally set up, the steam flow to the steam nozzle was to be measured by a turbine flowmeter rated for steam service. However, it was found that failure of the ball bearings occurred after only a few minutes steam flow, and replacement bearings also failed. The steam flowmeter was, therefore, discarded and the steam flow was calculated from the nozzle temperature and pressure measurements under the assumption of isentropic flow in the nozzle.

As a starting point for the condensation, it was desired that the steam entering the condenser test section be dry and saturated (a quality of 100 percent). To satisfy this condition for a given static pressure and steam velocity at the nozzle exit, the required pressure and temperature at the entrance of the nozzle were calculated with the aid of a Mollier chart under the assumption of isentropic nozzle flow. These required conditions were obtained by throttling the supplied high-pressure steam.

At the start of a test, the valve in the high-pressure steam line to the top of the settling tank was opened and the pressure in the tank was controlled by adjusting a valve which permitted the steam to escape to the atmosphere. The waterpump was then started and the flow valve adjusted to obtain the desired entering water velocity, as indicated by the flowmeter. The steam flow was next started gradually, and the throttling valves, in conjunction with the valves controlling the settling-tank pressure and the water velocity, were adjusted. This adjustment was a tedious process because of interactions between the controls, the time required for temperatures to stabilize, and occasional variations in steam-supply pressure. Cooling of the water by the heat exchanger could not be controlled closely enough to fix the entering-water temperature near a desired value; therefore, the water temperature was allowed to increase slowly, and data were recorded at several water inlet temperatures after the desired steam and water flow conditions had been reached. The condensation length was determined by visual observation of the test section.

RESULTS AND DISCUSSION

The data obtained in each test and the quantities computed from these data are given in table I in U.S. Customary Units and are repeated in table II in the International System of Units. Data are presented only for the three smallest diameter steam nozzles of the four tested. No measurements were obtained with the largest diameter steam nozzle because sufficiently steady flow could not be obtained within the operating limits of the present test loop.

Wall Measurements

The data of tables I and II are based on measurements of flow quantities made ahead of and behind the test section in which the condensation took place. In addition to these overall measurements, temperatures and static pressures along the glass test-section wall were measured for tests made with the steam nozzles of 0.418-in. (1.062-cm) and 0.316-in. (0.803-cm) inside diameter. Typical of these latter measurements are the data shown in figures 4 and 5 for the steam nozzles of 0.418-in. (1.062-cm) inside diameter and 0.316-in. (0.803-cm) inside diameter, respectively.

In addition to the plots of wall temperature and static pressure, figure 4 includes photographs of condensation taking place in the test section. The condensation region is indicated by the white area in the test section, the flow being from left to right. The effect of increasing inlet water temperature $T_{i,l}$ on the condensation length, wall temperatures, and static pressures is shown. In figure 4(a) the entering water temperature $T_{i,l}$ was relatively low, and the steam was completely condensed in the first inch (2.5 cm) of test section. At the wall, pressure and temperature rose sharply in the first 2 in. (5.1 cm) of the test section and remained nearly constant thereafter. The flow resulted in a positive pressure recovery so that the static pressure at the test-section exit was considerably greater than the static pressure of the entering steam.

In figure 4(b) the entering water was warmer than the water of figure 4(a), and the condensation length increased to nearly 6 in. (15.2 cm). The wall temperatures and pressures increased along the test section until the end of the condensation region and remained nearly constant thereafter. The entering water was only slightly warmer in figure 4(c) than in figure 4(b), but the condensation length increased greatly, from about 6 in. (15.2 cm) to about 20 inches (50.8 cm). This increase indicates that the water inlet temperature was approaching the condition at which the heat absorption capacity of the water would just equal the heat of condensation of the steam; for this condition the condensation length would approach infinity. In spite of the long condensation length, most of the water temperature rise occurred in the first few inches of the test section, indicating that this was the region of a high rate of heat transfer and condensation.

Figure 4(c) indicates that the water temperature leaving the test section was not limited to the temperature of the entering steam. The measured wall temperature was 216° F (376° K) whereas the entering steam temperature, corresponding to saturation temperature at an absolute pressure of 15 lbf/in^2 (103 kN/m^2), was 213° F (374° K). This condition was made possible by the pressure recovery experienced by the flow.

Similar wall-temperature and static-pressure data for the next smaller steam nozzle of 0.316-in. (0.803-cm) inside diameter are shown in figure 5 for several values of inlet water temperature. No photographs were made for this configuration; however, the end of the condensing region is indicated in each plot. For the shorter-condensation lengths, the wall temperature reached a maximum value a short distance downstream of the condensation region, then gradually decreased farther downstream to the final temperature. This occurrence of a temperature peak is not understood. In the previously discussed case of the 0.418 in. (1.062-cm) inside-diameter steam nozzle, the peak was much less evident (fig. 4). In the case of the smallest steam nozzle no information was obtained on the wall temperature.

When the condenser was operating at the longer condensation lengths, the length was very sensitive to small changes in test conditions. An extreme example of this sensitivity is shown by a comparison of figure 5(c) with 5(d), in which the condensation length more than doubles with no measured increase in the entering water temperature or apparent change in other test conditions. At this longest condensation length a critical operating condition had been reached at which any appreciable increase in inlet water temperature would have extended the condensation region into the diffuser and settling tank. The differences between the results shown in figures 5(c) and 5(d) were probably due to random errors in measurement and setting of the test conditions, which combined to produce a large change in condensation length.

The wall pressure data of figure 5 for the two longest condensation lengths show a decrease in static pressure for the first few inches of test section. This decrease suggests that the water flow velocity increased before slowing down at the end of the condensation region. Such a pressure variation is consistent with the shape of the typical condensation region observed in these tests. Photographs of the condensation taking place were not made for the operating conditions of figure 5, but some were obtained later at a lower steam velocity with a test section not instrumented with thermocouples and pressure orifices. These photographs are shown in figure 6 for the steam nozzle of 0.316-in. (0.803-cm) inside diameter, the same nozzle used for the data of figure 5, and also for the smallest nozzle tested, the nozzle of 0.158-in. (0.401-cm) inside diameter. The photographs show that the steam jet expanded after leaving the nozzle. Apparently, the water accelerated in this region of diminishing water passage area and dropping static pressure.

Stability of Flow

The data presented in this report were obtained with the condenser operating at steady or near-steady conditions. However, many operating conditions were encountered in which the flow was so rough, or in which regular oscillations of the flow and of the length of the condensation region were such that acceptable data for these conditions could not be obtained.

Preliminary tests of the condenser test loop were made with the 0.316-in. (0.803-cm) inside-diameter nozzle, one of the smaller nozzles tested. At water velocities below 20 ft/sec (6.1 m/s), with condensation taking place, the flow oscillated or surged strongly. This motion set the lower limit of inlet water velocity. At higher water velocities the flow improved in that the regular oscillations ceased, but the flow was often characterized by a random roughness as evidenced by a rapid and irregular changing of the condensation length of as much as 0.2 in. (±0.5 cm) and by some unsteadiness of the pressure indicators. Data obtained with this degree of flow roughness, however, were considered acceptable, the condensation length being taken as the mean length.

When the next larger steam nozzle of 0.418-in. (1.062-cm) inside diameter was tested, large regular fluctuations of the flow and condensation length occurred at some inlet water temperatures for all water velocities. At one particularly bad operating condition the flow surged strongly and regularly at about 3 cycles per second with the condensation length changing from 0 to 6 in. (15.2 cm). At other operating conditions, the condensation-length fluctuation shifted to a higher frequency (about 10 cycles per second) and lower amplitude. These instabilities were not encountered with this nozzle at water inlet temperatures high enough to result in condensation lengths greater than 5 in. (12.7 cm) nor were they always found when the condenser was operating at shorter condensation lengths. Data were not recorded at operating conditions which resulted in this surging flow.

As mentioned earlier, no useful data were obtained for the largest steam nozzle of 0.500-in. (1.270-cm) inside diameter because sufficiently steady flow could not be obtained within the operating limits of the present test loop. For this nozzle, surging with a frequency of about 2 to 3 cycles per second and condensation-length variations of several inches occurred for nearly every operating condition. A stable operating condition could be established with this nozzle if the inlet-water temperature were increased enough to result in a long condensation region; however, when this point was reached, the condensation region extended nearly the length of the test section so that the stable region of operation could not be explored. The high water temperature entering this particular pump at this condition soon resulted in cavitation, which prevented data from being obtained for this nozzle. Stable operation with this nozzle was, however, demonstrated and presumably could have been maintained if the flow had been cooled before reaching the pump.

The smallest nozzle tested had an inside diameter of 0.158 in. (0.401 cm). The flow with this nozzle tended to have a random unsteadiness or roughness which varied with initial water temperature. It was usually necessary to operate at inlet water temperatures above 180° F in order to produce acceptably smooth flow.

Experience in operating the jet condenser with these four nozzles indicates that the flow stability was improved by operating at inlet water velocities above 20 ft/sec (6.1 m/s). At a given inlet water velocity, stability could be improved by operating at a high inlet water temperature, which increased the length of the condensation region. Apparently, a very high rate of heat transfer per unit area of vapor-liquid interface may result in an unstable interface.

Condensation Length

In order to design a jet condenser for operation as part of a space power plant, an estimate of the condensation length is needed. In the present tests, with a slightly diverging test section, condensation length was affected by the water temperature and velocity, steam static pressure and velocity, and steam-nozzle size. A means of correlating the effects of these variables on the condensation length was sought. Correlation based on the correlating factor which had been used in part II of reference 1 was first attempted, but without success.

As a first step in a further attempt at correlation, the condensation-length data were plotted as a function of a temperature-rise parameter $\left(\frac{T_f - T_i}{T_{max} - T_i}\right)_l$ in which T_{max} is the saturation temperature of water at the pressure measured in the diffuser section downstream of the glass test section. The temperature T_{max} then represents the maximum temperature at which water could exist as a liquid at the final station in the condenser. The temperature-rise parameter represents the ratio of the water temperature rise produced by the condensation process to the maximum possible water temperature rise at the existing downstream pressure. These data, shown in figure 7, indicate that the condensation length increased rapidly with the temperature-rise parameter. At a given value of the temperature-rise parameter, increasing the water velocity increased the condensation length, whereas increasing the steam velocity decreased the condensation length.

Comparison of figures 7(a), 7(b), and 7(c) indicates the effects of an increase in the steam nozzle diameter (which at the same time reduces the water nozzle flow area). At a given value of the temperature-rise parameter, an increase in the steam nozzle size reduced the condensation length. For the smallest steam nozzle, the value of the temperature-rise parameter tended to be very low (fig. 7(a)) and thus indicated that this configuration could not nearly utilize the heat absorption capability of the water flow.

Comparison of figures 7(c) and 7(d) indicates the effect of a change in the steam static pressure. At a given value of the temperature-rise parameter, a decrease in the steam static pressure increased the condensation length.

It may be noted that seldom did the condensation length much exceed 13 in. (33 cm), and the condensation length of the smallest nozzle did not even approach this length. Condensation length was limited, not by the length of the glass test section, but by the capability of the test loop to maintain the static pressure of the entering steam at the desired fixed value. The condensation region tended to expand, as well as lengthen, as the temperature of the incoming water increased, and it became necessary to decrease the pressure in the settling tank to maintain the desired steam static pressure at the nozzle outlet. Eventually, a point was reached beyond which a reduction in tank pressure merely lengthened the condensation region without affecting the upstream static pressure. By the time this end point was reached, the diameter of the condensation region had expanded to nearly fill the glass test section.

Plotting the condensation-length data yielded a family of curves having the same general shape and having an apparently regular variation with water velocity. (See fig. 7.) The next step in correlation of the data was to find empirical relations to express the changes in the experimental curves produced by changing the variables of water velocity, steam velocity, steam pressure, and nozzle area. It was assumed for these tests that the condensation length was primarily a function of the temperature-rise parameter, the difference between the initial steam and water velocities, the water velocity, the specific volume of the entering steam, and the ratio of nozzle areas for liquid and vapor flow. By trial and error an empirical power (based on a power of 1.0 for the temperature-rise parameter) was found by which to raise each of these parameters to best fit the experimental condensation-length data. The best fit was obtained with the correlation factor

$$F = \left(\frac{T_f - T_i}{T_{max} - T_i}\right)_l \left[\frac{V_l^{3/2}}{\left(V_v - V_l\right)^{1/2}}\right]_i \left(\frac{A_l}{A_v}\right)^{0.9} v_{i,v}$$

in which the first term is the temperature-rise parameter; the second term is the ratio of the initial liquid velocity, raised to the 3/2 power, to the square root of the difference between the initial velocities of the vapor and the liquid; the third term is the ratio, raised to the 0.9 power, of the liquid nozzle area to the vapor nozzle area; and the last term is the specific volume of the entering vapor.

The measured condensation lengths plotted against this correlation factor are shown in figure 8. Although considerable scatter is present, the factor F can be used for a rough correlation of the data.

Power Required

As part of the jet condenser, a pump is used to circulate the liquid which condenses the vapor. The pumping power required to overcome the flow losses in the condenser has been computed as the product of the liquid-nozzle volume flow and the total-pressure loss measured from the inlet of the liquid nozzle to the diffuser downstream of the test section. These power data are given in tables I and II. The power required has also been made nondimensional by dividing it by the power equivalent of the heat of condensation of the vapor. These data are also given in the tables.

As mentioned previously, with increasing water inlet temperature, other inlet conditions being held constant, the condensation region tended to expand and increase in length. This increase resulted in a larger total-pressure drop (greater flow losses) and, therefore, more power required to pump the water. Since the power required increased with condensation length, the power ratio has been plotted against condensation length in figure 9. The increase of power-required ratio with condensation length appears to be linear. Increasing the steam velocity reduces the power-required ratio, the energy of the steam aiding the water flow.

The power-required-ratio data of figure 9 for a steam pressure of 15 lbf/in^2 (103 kN/m^2) have been cross-plotted in figure 10 for a steam velocity of 800 ft/sec (244 m/s) at a condensation length of 3.6 in. (9.1 cm). The curves indicate a rapid increase in the power-required ratio as the water inlet velocity increases. The power-required ratio for the smallest steam nozzle is seen to be relatively large because of the small heat content of its very limited steam flow. The pumping power required may be reduced by operating the condenser at a low water velocity with a large steam nozzle. However, fluctuating flow may be experienced if the operating velocity is too low.

To indicate the effect of steam static pressure on the power-required ratio, the data presented in figures 9(c) and 9(d) have been cross-plotted in figure 11. No pronounced effect is evident.

Pressure Augmentation

If a direct condenser, which combines the functions of a condenser and radiator, is used with a Rankine system, a pressure drop may occur in the flow through the condenser, and the boiler feed pump may experience cavitation. With the jet condenser, however, it is possible, by means of the pumped liquid flow, to increase the pressure of the condensate to more than offset the loss to be expected in the radiator and other piping. The measured pressure augmentation is shown in figure 12 as the ratio of the static-pressure rise to the dynamic pressure of the entering vapor. The static-pressure rise can be several times the vapor dynamic pressure, but as the condensation length increases, the pressure rise decreases because of the greater flow losses.

Some of the pressure-rise data of figure 12 have been cross-plotted in figure 13 for a steam velocity of 800 ft/sec (244 m/s) and a condensation length of 3.6 in. (9.1 cm). The pressure rise increases with inlet water velocity to more than five times the vapor dynamic pressure at the highest test water velocity of 60 ft/sec (18 m/s). The size of the steam nozzle is seen to have little effect on the pressure rise experienced by the condensate.

Evidently, a large pressure rise comes about because power is expended in pumping the flow. This pressure rise is illustrated by figure 14 in which the pressure-rise data of figure 13 are plotted against the corresponding values of the power-required ratio taken from figure 10. For a given power ratio and condensation length the greatest pressure rise is obtained with the largest steam nozzle. Thus, a relatively large ratio of steam nozzle area to water nozzle area is more efficient in that pressure augmentation is accomplished with less pumping power per unit steam flow.

CONCLUDING REMARKS

An exploratory ground-based investigation has been made of a jet condenser of a type for which operation should be little affected by gravitational forces. Steam was condensed by water, the steam entering the condenser through a central nozzle and water entering through a surrounding annular nozzle. The steam and water flowed horizontally through a condenser tube, condensation of the steam occurring through direct contact with the water.

The condensation length was affected by the flow variables and nozzle configuration. An empirical parameter, based on the flow conditions and nozzle area ratio, was found to correlate roughly the experimental condensation-length data.

The jet condenser offers a means of pressure augmentation of the condensate through the expenditure of pumping power. The jet condenser was able to increase the static pressure of the condensate by an amount several times the vapor dynamic pressure. A relatively large ratio of steam nozzle area to water nozzle area was found to be more efficient in that pressure augmentation was accomplished with less pumping power required per unit steam flow; however, a large nozzle area ratio increased the possibility of developing regular fluctuations of the flow, accompanied by oscillations of the condensation length. These oscillations could be avoided by operation at higher water inlet temperatures, which increased the condensation length, but which also increased the flow losses. These results indicate that the jet condenser investigated (inner vapor nozzle, outer liquid nozzle) is feasible for space application although the range of stable operation is limited.

Langley Research Center,
National Aeronautics and Space Administration,
Langley Station, Hampton, Va., May 28, 1965.

APPENDIX

CONVERSION OF U.S. CUSTOMARY UNITS TO SI UNITS

The International System of Units (SI) was adopted by the Eleventh General Conference on Weights and Measures, Paris, October 1960, in Resolution No. 12 (ref. 3). Conversion factors for the units used herein are given in the following table:

Physical quantity	U.S. Customary Unit	Conversion factor*	SI unit
Force	lbf	4.448	newtons (N)
Heat-transfer rate	Btu/hr	0.2933	watts (W)
Length	in.	0.0254	meters (m)
	ft	0.3048	meters (m)
Mass	lbm	0.4536	kilograms (kg)
Power	ft-lbf/sec	1.356	watts (W)
Pressure	lbf/in^2	6895	newtons/meter^2 (N/m^2)
Temperature	$^{\circ}$F + 460	5/9	degrees Kelvin ($^{\circ}$K)

*Multiply value given in U.S. Customary Unit by conversion factor to obtain equivalent value in SI units.

Prefixes to indicate multiple of units are as follows:

Prefix	Multiple
kilo (k)	10^3
centi (c)	10^{-2}

REFERENCES

1. Hays, Lance: Investigation of Condensers Applicable to Space Power Systems. Part I - Direct Condensers, Rept. 1588-Final (Contract NAS7-11), Electro-Optical Systems, Inc., Aug. 15, 1962.
   Part II - Jet Condensers, Rept. 1588-Final II (Contract NAS7-11), Electro-Optical Systems, Inc., Nov. 30, 1962.

2. Kemper, C. A.; and Brown, G. A.: The Condensing-Ejector Refrigeration System for Space Vehicles. Proceedings of the First Space Vehicle Thermal and Atmospheric Control Symposium. ASD-TDR-63-260, U.S. Air Force, Apr. 1963, pp. 673-708.

3. Mechtly, E. A.: The International System of Units - Physical Constants and Conversion Factors. NASA SP-7012, 1964.

TABLE I.- TEST DATA (U.S. CUSTOMARY UNITS)

$V_{i,l}$, ft/sec	$T_{i,l}$, °F	$T_{f,l}$, °F	l, in.	$p'_{i,l}$, lbf/in^2	$p'_{f,l}$, lbf/in^2	$T_{max,l}$, °F	$\left(\frac{T_f - T_i}{T_{max} - T_i}\right)_l$	F, ft^4/lbm-sec	$\frac{p_{f,l} - p_{i,v}}{q_{i,v}}$	P_r, ft-lbf/sec	P_r/P_c	w_l/w_v
Nozzle i.d. = 0.158 in.; A_v/A_l = 0.081; $p_{i,v}$ = 15 lb/in^2; $V_{i,v}$ = 600 ft/sec; Q = 10 450 Btu/hr												
20	184.5	186.0	1.5	17.9	16.7	218.2	0.045	42.3	1.17	6.1	0.0027	655
	191.2	192.6	1.9	18.0	16.6	218.1	.056	52.8	1.03	6.5	.0029	649
	194.7	195.7	6.2	17.8	15.5	214.8	.075	70.4	.42	10.7	.0047	649
	195.4	196.1	2.9	18.0	16.4	217.3	.069	64.9	.94	7.5	.0033	649
30	190.9	191.6	2.1	21.4	18.9	224.8	.030	51.8	2.58	17.5	.0077	976
	195.4	196.0	3.1	21.6	18.8	224.5	.034	59.9	2.58	19.6	.0087	976
	196.7	198.2	6.4	21.4	17.8	221.7	.040	69.9	1.83	25.2	.0111	976
45	184.2	184.7	1.7	29.8	23.9	237.4	.013	40.5	6.14	61.9	.0274	1470
	189.0	190.3	2.0	30.1	24.1	237.9	.014	43.9	6.08	63.0	.0279	1470
	197.5	198.0	2.9	29.9	23.8	237.0	.017	54.7	6.00	64.1	.0284	1460
	199.5	200.8	7.7	29.6	22.3	233.6	.020	63.3	4.93	77.6	.0343	1460
Nozzle i.d. = 0.158 in.; A_v/A_l = 0.081; $p_{i,v}$ = 15 lbf/in^2; $V_{i,v}$ = 800 ft/sec; Q = 13 900 Btu/hr												
20	184.8	186.4	1.3	17.9	16.8	218.6	0.060	48.6	0.69	5.1	0.0017	491
	191.3	193.5	1.8	18.0	16.8	218.6	.074	59.6	.69	5.6	.0019	488
	194.3	196.5	3.2	17.9	16.3	217.3	.087	70.7	.50	7.5	.0025	488
	195.5	196.7	7.3	17.7	15.3	214.3	.106	86.2	.11	11.2	.0037	488
30	184.8	186.5	1.8	21.5	18.9	224.9	.034	50.5	1.53	18.2	.0060	740
	192.3	194.5	4.9	21.7	18.1	222.4	.044	66.5	1.22	25.2	.0084	736
45	178.7	180.0	1.6	30.1	24.3	238.4	.015	41.5	3.49	60.9	.0202	1106
	186.5	187.3	1.8	30.1	24.3	238.2	.017	47.8	3.49	60.9	.0202	1106
	192.6	193.0	2.6	29.8	24.1	237.8	.020	54.1	3.49	60.9	.0202	1100
	194.2	195.0	8.2	29.8	22.0	232.9	.023	63.4	2.66	81.9	.0272	1100
Nozzle i.d. = 0.316 in.; A_v/A_l = 0.472; $p_{i,v}$ = 15 lbf/in^2; $V_{i,v}$ = 800 ft/sec; Q = 57 300 Btu/hr												
30	137.6	145.0	0.6	22.0	20.2	228.5	0.080	24.5	2.01	8.9	0.0007	128
	165.8	173.0	1.9	21.1	19.8	227.5	.117	35.8	1.87	6.4	.0005	127
	170.0	176.7	2.0	21.7	19.6	226.9	.118	36.3	1.88	10.4	.0008	127
	170.3	177.8	2.1	21.7	19.9	227.7	.131	40.2	1.90	8.9	.0007	127
	[a]178.0	185.4	2.9	21.9	19.8	227.4	.160	48.9	1.82	10.4	.0008	127
	[a]184.3	191.3	3.5	22.1	19.9	227.5	.181	55.4	1.88	10.9	.0008	127
	[a]188.5	196.0	4.1	22.1	19.6	226.8	.204	65.2	1.75	11.9	.0009	126
	[a]191.7	199.5	5.1	22.1	19.2	225.6	.230	70.7	1.56	14.4	.0011	126
	192.2	199.0	4.2	22.1	19.4	226.3	.199	61.0	1.60	13.3	.0011	126
	[a]192.7	201.0	16.3	21.7	16.1	216.5	.327	100.3	.42	28.1	.0022	126
	[a]193.5	201.3	9.9	22.1	17.7	221.4	.278	85.4	.95	21.7	.0017	126
45	150.0	154.5	.8	30.6	25.2	240.4	.050	28.1	3.81	39.8	.0032	192
	172.6	177.6	2.2	30.4	24.7	239.3	.075	42.1	3.62	42.1	.0034	190
	178.0	182.8	2.7	29.5	23.8	237.2	.081	45.8	3.50	42.1	.0034	190
	193.6	198.7	4.5	29.9	23.4	236.3	.119	67.3	3.20	48.0	.0039	189
	194.5	199.7	6.0	30.0	22.7	234.6	.130	73.3	2.94	53.9	.0044	189
60	152.6	156.0	1.0	42.0	31.6	253.1	.034	30.0	6.60	102.5	.0084	256
	172.5	176.4	2.1	40.7	29.9	250.2	.050	44.2	5.65	106.4	.0085	254
	187.0	191.2	3.2	41.8	30.1	252.2	.064	61.8	5.72	115.4	.0085	252
	191.8	195.7	8.9	41.6	26.4	243.2	.076	67.2	4.34	149.9	.0120	252
Nozzle i.d. = 0.316 in.; A_v/A_l = 0.472; $p_{i,v}$ = 15 lbf/in^2; $V_{i,v}$ = 1100 ft/sec; Q = 78 800 Btu/hr												
20	148.7	165.8	0.8	17.9	19.0	225.2	0.224	31.5	0.82	-3.6	-0.0002	62
	170.5	187.0	1.6	17.8	18.8	224.6	.305	42.9	.76	-3.3	-.0002	61
	179.9	196.0	2.4	17.6	18.3	223.2	.372	52.6	.73	-2.3	-.0001	61
	184.0	200.4	13.0	17.7	15.4	214.3	.542	76.5	.10	7.5	.0004	61
30	152.2	162.1	.8	23.5	21.9	232.7	.123	31.5	1.37	7.9	.0005	93
	179.0	189.7	2.5	23.2	21.5	231.7	.203	53.1	1.27	8.4	.0005	92
	190.5	200.5	13.5	23.0	17.4	220.5	.333	85.4	.44	27.6	.0016	92
	191.0	201.1	5.9	22.9	20.1	228.2	.272	71.0	1.03	13.8	.0008	91
45	147.0	153.5	.6	29.8	26.0	242.2	.068	32.6	2.25	28.0	.0016	140
	168.3	175.6	1.9	29.8	25.8	241.7	.099	47.3	2.20	29.5	.0017	139
	171.7	178.3	2.0	29.4	25.6	241.3	.095	45.2	2.18	28.0	.0016	139
	183.9	190.7	3.2	29.7	25.4	240.8	.119	56.8	2.10	31.8	.0025	138
	191.7	198.8	13.8	29.9	20.8	230.0	.186	88.5	1.19	67.3	.0053	138
60	145.7	151.2	.6	42.0	33.4	256.5	.050	36.8	3.71	84.6	.0050	186
	169.0	174.9	1.7	39.8	32.0	253.9	.069	51.2	3.42	77.0	.0045	185
	185.0	190.6	3.0	41.8	31.9	253.8	.081	60.5	3.43	97.5	.0057	184
	191.5	196.3	12.5	40.2	25.3	240.6	.098	73.0	2.16	146.8	.0086	183

[a]Checkpoints made near end of investigation.

TABLE I.- TEST DATA (U.S. CUSTOMARY UNITS) - Concluded

$V_{i,l}$, ft/sec	$T_{i,l}$, °F	$T_{f,l}$, °F	l, in.	$p'_{i,l}$, lbf/in²	$p'_{f,l}$, lbf/in²	$T_{max,l}$, °F	$\left(\frac{T_f - T_i}{T_{max} - T_i}\right)_l$	F, ft⁴/lbm-sec	$\frac{p_{f,l} - p_{i,v}}{q_{i,v}}$	P_r, ft-lbf/sec	P_r/P_c	w_l/w_v
Nozzle i.d. = 0.418 in.; A_v/A_l = 1.37; $p_{i,v}$ = 10 lbf/in²; $V_{i,v}$ = 800 ft/sec; Q = 69 700 Btu/hr												
30	168.9	183.7	6.2	17.3	13.7	208.3	0.376	64.2	2.01	10.8	0.0007	64
	173.8	189.4	11.5	16.6	12.6	204.2	.513	87.9	1.39	11.9	.0008	64
45	153.7	164.4	2.7	26.1	17.7	221.4	.158	49.5	4.21	37.7	.0025	96
	167.1	178.0	4.6	25.6	16.9	219.0	.210	65.9	3.81	39.0	.0026	96
	172.8	183.1	6.3	26.0	16.4	217.4	.231	72.6	3.51	43.0	.0029	96
60	146.0	154.0	1.6	38.8	23.6	236.8	.088	43.3	7.45	90.8	.0060	129
	160.3	167.3	3.3	37.8	21.5	231.7	.098	48.1	6.49	97.5	.0065	129
	164.0	171.4	3.5	38.2	22.0	232.9	.107	52.7	6.60	96.6	.0064	128
	172.8	179.8	5.2	39.0	21.4	231.4	.119	58.6	6.29	105.3	.0070	128
	173.2	180.8	5.2	38.4	21.3	231.2	.131	64.6	6.21	102.0	.0068	128
Nozzle i.d. = 0.418 in.; A_v/A_l = 1.37; $p_{i,v}$ = 10 lbf/in²; $V_{i,v}$ = 1100 ft/sec; Q = 95 700 Btu/hr												
30	118.4	139.4	0.5	17.0	15.8	215.6	0.216	31.4	1.82	3.6	0.0002	48
	160.6	182.8	3.3	17.0	15.8	215.6	.404	58.8	1.67	3.6	.0002	47
	170.3	192.0	5.8	17.5	15.1	213.6	.505	73.3	1.47	7.2	.0003	47
	171.2	192.7	6.6	17.1	14.7	211.9	.528	76.5	1.35	7.2	.0003	47
45	133.4	147.0	.7	27.2	19.7	227.2	.145	38.6	2.82	33.6	.0016	71
	152.0	166.1	1.9	27.4	19.5	226.5	.190	50.4	2.82	35.4	.0017	70
	168.0	181.9	3.4	28.1	19.1	225.5	.242	64.5	2.67	40.3	.0019	70
	172.2	186.3	4.2	28.9	19.1	225.2	.266	70.9	2.68	43.9	.0021	70
	173.0	187.3	8.0	28.4	16.7	218.4	.315	83.8	1.97	52.4	.0025	70
60	156.8	167.3	1.7	42.3	26.9	244.0	.121	50.1	4.96	92.9	.0045	93
	158.1	168.9	1.9	41.6	26.9	244.0	.126	52.1	4.98	87.9	.0042	93
	170.2	180.4	2.8	41.3	27.0	244.2	.138	57.3	4.98	85.5	.0041	93
	170.4	180.6	3.3	41.2	26.3	242.7	.141	58.4	4.78	89.1	.0043	93
	176.3	186.5	6.6	38.6	21.4	231.5	.185	76.5	3.33	102.8	.0050	93
Nozzle i.d. = 0.418 in.; A_v/A_l = 1.37; $p_{i,v}$ = 15 lbf/in²; $V_{i,v}$ = 800 ft/sec; Q = 100 600 Btu/hr												
30	142.5	162.1	1.1	21.4	19.6	226.9	0.232	27.2	1.90	5.4	0.0002	44
	152.8	171.9	1.5	21.2	19.3	226.1	.260	30.7	1.67	5.7	.0003	44
	180.7	204.0	5.0	22.0	19.5	226.5	.509	59.6	1.67	7.5	.0003	44
	188.0	211.0	8.4	21.9	18.8	224.6	.629	74.0	1.40	9.3	.0004	44
	189.9	212.0	12.2	22.0	18.1	222.7	.674	79.0	1.19	11.7	.0005	43
45	149.2	163.7	1.0	32.4	23.8	237.3	.165	35.7	3.28	38.5	.0018	66
	188.3	203.7	5.1	32.7	22.6	234.4	.324	69.9	2.86	45.2	.0021	65
	191.5	206.0	7.1	33.4	21.5	231.7	.361	77.8	2.49	53.3	.0025	65
	193.2	207.7	9.0	33.5	20.6	229.5	.400	86.2	2.14	57.7	.0026	65
	193.9	208.0	12.9	32.7	19.2	225.8	.442	95.8	1.56	60.5	.0028	65
60	180.8	192.0	2.7	53.5	30.0	250.2	.161	54.5	5.56	140.4	.0065	87
	187.7	198.8	3.7	53.1	29.4	249.0	.181	61.2	5.50	141.6	.0065	87
	195.0	206.1	5.5	53.5	28.0	246.4	.216	73.4	4.93	152.2	.0070	87
	196.9	208.4	9.4	55.3	25.8	241.7	.257	86.6	4.08	176.4	.0081	87
Nozzle i.d. = 0.418 in.; A_v/A_l = 1.37; $p_{i,v}$ = 15 lbf/in²; $V_{i,v}$ = 1100 ft/sec; Q = 138 500 Btu/hr												
30	131.4	162.1	0.7	22.3	22.4	233.9	0.300	29.9	1.40	-0.3	0	32
	178.2	210.2	3.9	21.8	21.8	232.5	.590	58.6	1.40	0	0	32
	183.0	215.1	5.3	22.0	21.5	231.7	.659	66.0	1.31	1.5	0	32
	185.9	217.7	8.1	21.8	20.6	229.5	.730	72.7	1.13	3.6	.0001	32
	186.7	218.3	20.2	22.0	18.7	224.4	.839	83.5	.77	9.9	.0003	32
45	164.0	182.2	1.9	32.8	25.6	241.3	.236	43.0	2.14	32.2	.0011	48
	179.9	200.9	3.4	32.5	25.1	240.2	.349	64.0	2.03	33.1	.0011	48
	181.5	203.0	3.6	32.6	25.2	240.4	.366	66.8	2.05	33.1	.0011	48
	188.0	209.0	5.2	33.3	24.6	239.5	.408	74.2	1.93	38.9	.0013	47
60	184.7	200.0	3.3	55.6	32.4	254.7	.219	62.7	3.39	138.7	.0046	63
	190.0	205.3	4.0	57.7	32.3	254.5	.237	67.3	3.47	152.0	.0051	63

TABLE II.- TEST DATA (INTERNATIONAL SYSTEM OF UNITS)

$V_{i,l}$, m/sec	$T_{i,l}$, °K	$T_{f,l}$, °K	l, cm	$p'_{i,l}$, kN/m²	$p'_{f,l}$, kN/m²	$T_{max,l}$, °K	$\left(\frac{T_f - T_i}{T_{max} - T_i}\right)_l$	F, m⁴/kg-s	$\frac{p_{f,l} - p_{i,v}}{q_{i,v}}$	P_r, W	P_r/P_c	w_l/w_v
Nozzle i.d. = 0.401 cm; A_v/A_l = 0.081; $p_{i,v}$ = 103 kN/m²; $V_{i,v}$ = 183 m/sec; Q = 3100 W												
6.1	358.0	358.9	3.8	123	115	376.8	0.045	0.81	1.17	8.3	0.0027	655
	361.8	362.6	4.8	124	114	376.7	.056	1.01	1.03	8.8	.0029	649
	363.7	364.3	15.7	123	107	374.9	.075	1.34	.42	14.5	.0047	649
	364.1	364.5	7.4	124	113	376.3	.069	1.24	.94	10.2	.0033	649
9.1	361.6	362.0	5.3	148	130	380.4	.030	.99	2.58	23.7	.0077	976
	364.1	364.4	7.9	.49	130	380.3	.034	1.14	2.58	26.6	.0087	976
	364.8	365.7	16.2	148	123	378.7	.040	1.33	1.83	34.2	.0111	976
13.7	357.9	358.2	4.3	205	165	387.4	.013	.77	6.14	83.9	.0274	1470
	360.6	361.3	5.1	208	166	387.7	.014	.84	6.08	85.4	.0279	1470
	365.3	365.6	7.4	206	164	387.2	.017	1.04	6.00	86.9	.0284	1460
	366.4	367.1	19.6	204	154	385.3	.020	1.20	4.93	105.2	.0343	1460
Nozzle i.d. = 0.401 cm; A_v/A_l = 0.081; $p_{i,v}$ = 103 kN/m²; $V_{i,v}$ = 244 m/sec; Q = 4100 W												
6.1	358.2	359.1	3.3	123	116	377.0	0.060	0.93	0.69	6.9	0.0017	491
	361.8	363.0	4.6	124	116	377.0	.074	1.13	.69	7.6	.0019	488
	363.5	364.7	8.1	123	112	376.3	.087	1.35	.50	10.2	.0025	488
	364.2	364.8	18.6	122	105	374.6	.106	1.64	.11	15.2	.0037	488
9.1	358.2	359.2	4.6	148	130	380.5	.034	.96	1.53	24.7	.0060	740
	362.4	363.6	12.4	150	125	379.1	.044	1.27	1.22	34.2	.0084	736
13.7	354.8	355.6	4.1	208	168	388.0	.015	.79	3.49	82.6	.0202	1106
	359.2	359.6	4.6	208	168	387.9	.017	.91	3.49	82.6	.0202	1106
	362.6	362.8	6.6	205	166	387.7	.020	1.03	3.49	82.6	.0202	1100
	363.4	363.9	20.8	205	152	384.9	.023	1.21	2.66	111.1	.0272	1100
Nozzle i.d. = 0.803 cm; A_v/A_l = 0.472; $p_{i,v}$ = 103 kN/m²; $V_{i,v}$ = 244 m/sec; Q = 16 800 W												
9.1	332.1	336.2	1.5	152	139	382.5	0.080	0.47	2.01	12.1	0.0007	128
	347.7	351.7	4.8	145	137	382.0	.117	.68	1.87	8.7	.0005	127
	350.0	353.7	5.1	150	135	381.7	.118	.69	1.88	14.1	.0008	127
	350.2	354.4	5.3	150	137	382.1	.131	.76	1.90	12.0	.0007	127
	[a]354.4	358.6	7.4	151	137	381.9	.160	.93	1.82	14.1	.0008	127
	[a]357.9	361.8	8.9	152	137	381.9	.181	1.05	1.88	14.8	.0008	127
	[a]360.3	364.4	10.4	152	135	381.6	.204	1.29	1.75	16.1	.0009	126
	[a]362.0	366.4	13.0	152	132	380.9	.230	1.35	1.56	19.5	.0011	126
	362.3	366.1	10.7	152	134	381.3	.199	1.16	1.60	18.0	.0011	126
	[a]362.6	367.2	41.4	150	111	375.8	.327	1.91	.42	38.1	.0022	126
	[a]363.0	367.4	25.1	152	122	378.6	.278	1.62	.95	29.4	.0017	126
13.7	339.0	341.4	2.0	211	174	389.1	.050	.54	3.81	54.0	.0032	192
	351.5	354.3	5.6	210	170	388.5	.075	.80	3.62	57.0	.0034	190
	354.5	357.2	6.9	203	164	387.3	.081	.87	3.50	57.0	.0034	190
	363.1	366.0	11.4	206	161	386.9	.119	1.28	3.20	65.0	.0039	189
	363.7	366.7	15.2	207	157	385.9	.130	1.40	2.94	73.0	.0044	189
18.3	340.4	342.3	2.5	290	218	396.2	.034	.57	6.60	139.0	.0084	256
	351.4	353.6	5.3	281	206	394.5	.050	.84	5.65	144.0	.0085	254
	359.5	361.8	8.1	288	208	395.7	.064	1.18	5.72	156.4	.0085	252
	362.1	364.3	22.6	287	182	390.7	.076	1.28	4.34	203	.0120	252
Nozzle i.d. = 0.803 cm; A_v/A_l = 0.472; $p_{i,v}$ = 103 kN/m²; $V_{i,v}$ = 335 m/sec; Q = 23 100 W												
6.1	338.2	347.7	2.0	123	131	380.7	0.224	0.60	0.82	-4.9	-0.0002	62
	350.3	359.5	4.1	123	130	380.4	.305	.82	.76	-4.5	-.0002	61
	355.5	364.5	6.1	121	126	379.6	.372	1.00	.73	-3.1	-.0001	61
	357.8	366.9	33.0	122	106	374.7	.542	1.46	.10	10.2	.0004	61
9.1	340.2	345.6	2.0	162	151	384.9	.123	.60	1.37	10.7	.0005	93
	355.0	361.0	6.4	160	148	384.3	.203	1.01	1.27	11.4	.0005	92
	361.4	367.0	34.3	159	120	378.1	.333	1.63	.44	37.4	.0016	92
	361.7	367.3	15.0	158	139	382.3	.272	1.35	1.03	18.7	.0008	91
13.7	337.3	340.9	1.5	205	179	390.1	.068	.62	2.25	38.0	.0016	140
	349.1	352.3	4.8	205	178	389.9	.099	.90	2.20	40.0	.0017	139
	351.0	354.7	5.1	203	177	389.6	.095	.86	2.18	38.0	.0016	139
	357.7	361.5	8.1	205	175	389.3	.119	1.08	2.10	43.1	.0025	138
	362.0	366.0	35.0	206	143	383.4	.186	1.68	1.19	91.1	.0053	138
18.3	336.5	339.6	1.5	290	230	398.0	.050	.70	3.71	114.6	.0050	186
	349.5	352.7	4.3	274	221	396.6	.069	.97	3.42	104.3	.0045	185
	358.4	361.5	7.6	288	220	396.5	.081	1.15	3.43	132	.0057	184
	362.0	364.7	31.8	277	174	389.2	.098	1.39	2.16	199	.0086	183

[a]Checkpoints made near end of investigation.

TABLE II.- TEST DATA (INTERNATIONAL SYSTEM OF UNITS) - Concluded

$V_{i,l}$, m/sec	$T_{i,l}$, °K	$T_{f,l}$, °K	l, cm	$p'_{i,l}$, kN/m^2	$p'_{f,l}$, kN/m^2	$T_{max,l}$, °K	$\left(\frac{T_f - T_i}{T_{max} - T_i}\right)_l$	F, m^4/kg-s	$\frac{p_{f,l} - p_{i,v}}{q_{i,v}}$	P_r, W	P_r/P_c	w_l/w_v
Nozzle i.d. = 1.062 cm; A_v/A_l = 1.37; $p_{i,v}$ = 69 kN/m^2; $V_{i,v}$ = 244 m/sec; Q = 20 400 W												
9.1	349.4	357.6	15.7	119	94	371.3	0.376	1.22	2.01	14.6	0.0007	64
	352.1	360.8	29.2	114	87	369.0	.513	1.67	1.39	16.1	.0008	64
13.7	340.9	346.9	6.8	180	122	378.6	.158	.94	4.21	51.1	.0025	96
	348.4	354.4	11.7	177	117	377.2	.210	1.25	3.81	52.9	.0026	96
	351.6	357.3	16.0	179	113	376.3	.231	1.38	3.51	58.3	.0029	96
18.3	336.7	341.1	4.1	268	163	387.1	.088	.82	7.45	123.1	.0060	129
	344.6	348.5	8.4	261	148	384.3	.098	.92	6.49	132.2	.0065	129
	346.7	350.8	8.9	263	152	384.9	.107	1.00	6.60	131.0	.0064	128
	351.6	355.4	13.2	269	148	384.1	.119	1.12	6.29	142.8	.0070	128
	351.8	356.0	13.2	265	147	384.0	.131	1.23	6.21	138.3	.0068	128
Nozzle i.d. = 1.062 cm; A_v/A_l = 1.37; $p_{i,v}$ = 69 kN/m^2; $V_{i,v}$ = 335 m/sec; Q = 28 100 W												
9.1	321.3	333.0	1.3	117	109	375.3	0.216	0.60	1.82	4.9	0.0002	48
	344.8	357.1	8.4	117	109	375.3	.404	1.12	1.67	4.9	.0002	47
	350.2	362.2	14.7	121	104	374.2	.505	1.40	1.47	9.8	.0003	47
	350.7	362.6	16.8	118	101	373.3	.528	1.46	1.35	9.8	.0003	47
13.7	329.7	337.2	1.8	188	136	381.8	.145	.73	2.82	45.6	.0016	71
	340.0	347.8	4.8	189	134	381.4	.190	.96	2.82	48.0	.0017	70
	348.9	356.6	8.6	194	132	380.8	.242	1.23	2.67	54.6	.0019	70
	351.2	359.0	10.7	199	132	380.7	.266	1.35	2.68	59.5	.0021	70
	351.7	359.6	20.3	196	115	376.9	.315	1.60	1.97	71.0	.0025	70
18.3	342.7	348.5	4.3	292	185	391.1	.121	.95	4.96	126.0	.0045	93
	343.4	349.4	4.8	287	185	391.1	.126	.99	4.98	119.2	.0042	93
	350.1	355.8	7.1	285	186	391.2	.138	1.09	4.98	115.9	.0041	93
	350.2	355.9	8.4	284	181	390.4	.141	1.11	4.78	120.8	.0043	93
	353.5	359.2	16.8	266	148	384.2	.185	1.46	3.33	139.4	.0050	93
Nozzle i.d. = 1.062 cm; A_v/A_l = 1.37; $p_{i,v}$ = 103 kN/m^2; $V_{i,v}$ = 244 m/sec; Q = 29 500 W												
9.1	334.8	345.6	2.8	148	135	381.6	0.232	0.52	1.90	7.3	0.0002	44
	340.5	351.1	3.8	146	133	381.2	.260	.58	1.67	7.7	.0003	44
	356.0	368.9	12.7	152	134	381.4	.509	1.13	1.67	10.1	.0003	44
	360.0	372.8	21.3	151	130	380.4	.629	1.41	1.40	12.1	.0004	44
	361.1	373.4	31.0	152	125	379.3	.674	1.50	1.19	15.8	.0005	43
13.7	338.5	346.5	2.5	223	164	387.4	.165	.68	3.28	52.2	.0018	66
	360.2	368.7	13.0	225	156	385.8	.324	1.33	2.86	61.2	.0021	65
	361.9	370.0	18.0	230	148	384.3	.361	1.48	2.49	72.3	.0025	65
	362.9	371.0	22.9	231	142	383.1	.400	1.64	2.14	78.2	.0026	65
	363.3	371.1	32.8	225	132	381.0	.442	1.82	1.56	82.0	.0028	65
18.3	356.0	362.2	6.9	369	207	394.5	.161	1.04	5.56	190.4	.0065	87
	359.8	366.0	9.4	366	203	393.9	.181	1.16	5.50	192.0	.0065	87
	363.9	370.0	14.0	369	193	392.4	.216	1.40	4.93	206.4	.0070	87
	364.9	371.3	23.9	381	178	389.8	.257	1.65	4.08	239.2	.0081	87
Nozzle i.d. = 1.062 cm; A_v/A_l = 1.37; $p_{i,v}$ = 103 kN/m^2; $V_{i,v}$ = 335 m/sec; Q = 40 600 W												
9.1	328.6	345.6	1.8	154	154	385.5	0.300	0.57	1.40	-0.4	0	32
	354.6	372.3	9.9	150	150	384.7	.590	1.12	1.40	0	0	32
	357.2	375.0	13.5	152	148	384.3	.659	1.26	1.31	2.0	0	32
	358.8	376.5	20.6	150	142	383.0	.730	1.38	1.13	4.9	.0001	32
	359.3	376.8	51.3	152	129	380.2	.839	1.59	.77	13.4	.0003	32
13.7	346.7	356.8	4.8	226	177	389.6	.236	.82	2.14	43.7	.0011	48
	355.5	367.2	8.6	224	173	389.0	.349	1.22	2.03	44.9	.0011	48
	356.4	368.3	9.1	225	174	389.1	.366	1.27	2.05	44.9	.0011	48
	360.0	371.7	13.2	230	170	388.6	.408	1.41	1.93	52.7	.0013	47
18.3	358.2	366.7	8.4	383	223	397.0	.219	1.19	3.39	188.1	.0046	63
	361.1	369.6	10.2	398	223	396.9	.237	1.28	3.47	206.1	.0051	63

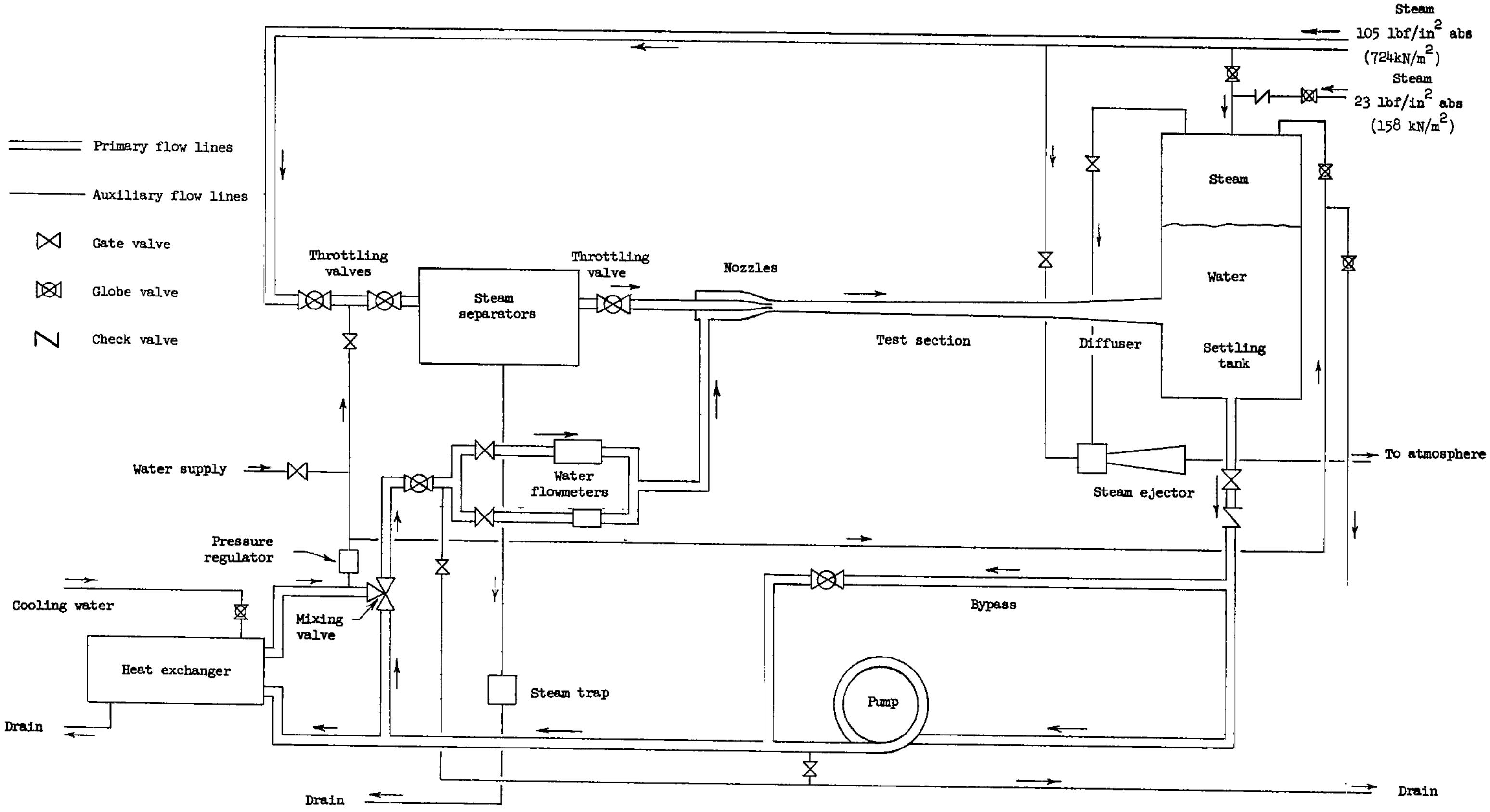

Figure 1.- Schematic of condenser flow system.

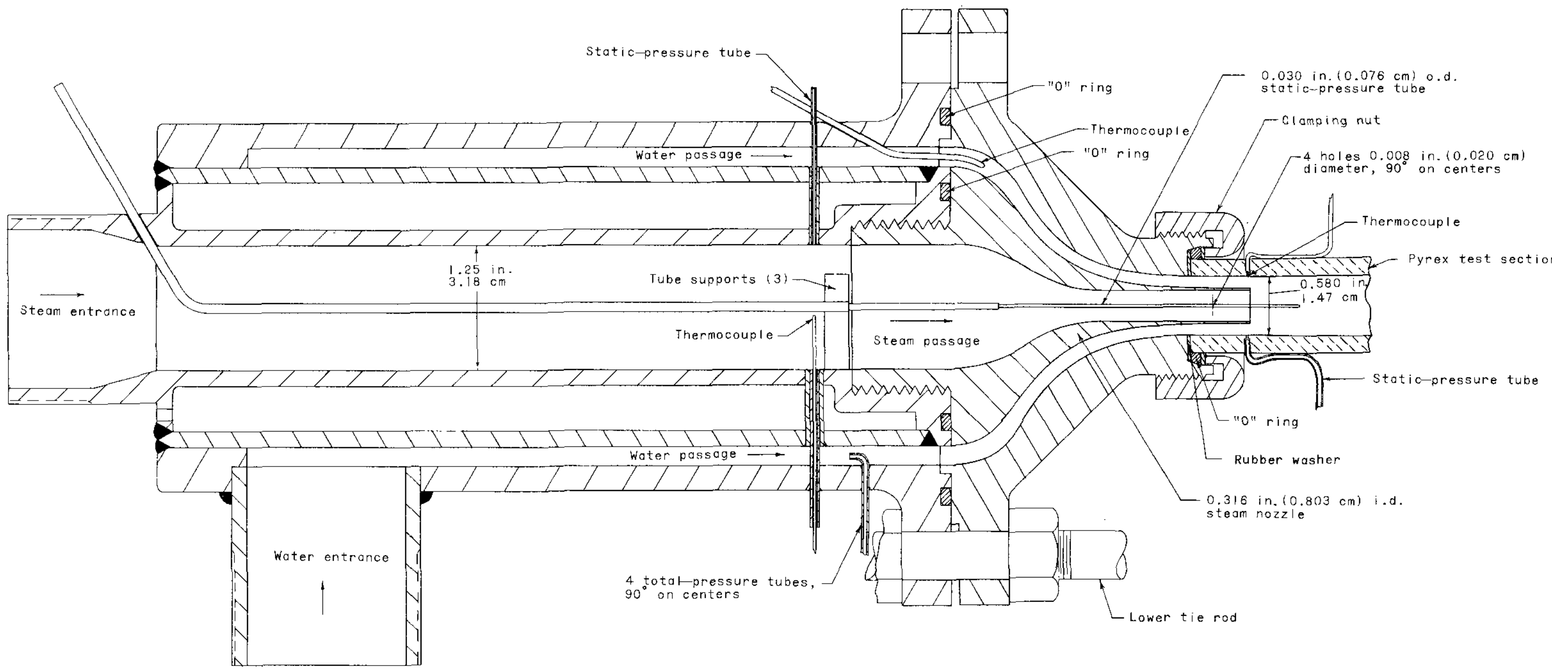

Figure 2.- Nozzle and test-section assembly.

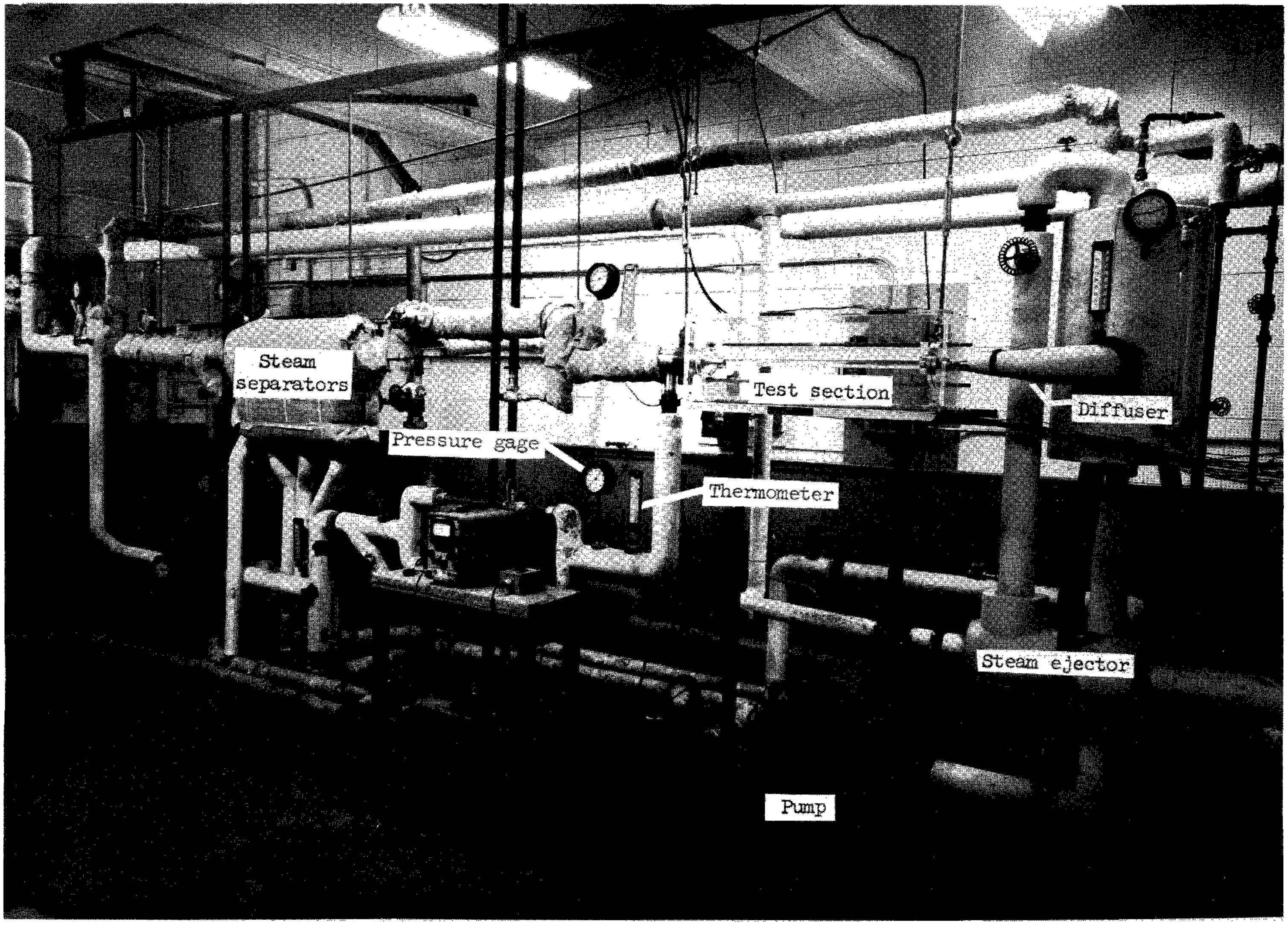

Figure 3.- Photograph of condenser flow system.

L-62-8916.1

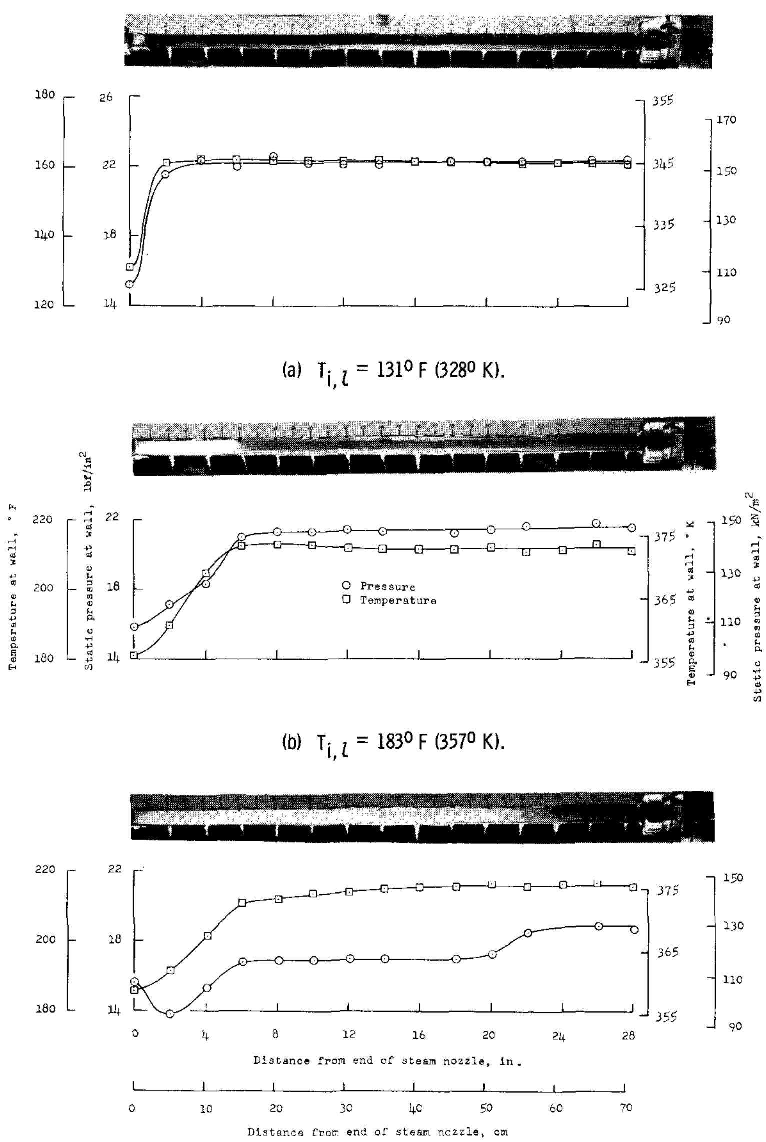

(a) $T_{i,l} = 131^{\circ}$ F (328° K).

(b) $T_{i,l} = 183^{\circ}$ F (357° K).

(c) $T_{i,l} = 187^{\circ}$ F (359° K).

L-65-142

Figure 4.- Typical temperature and pressure distributions along test-section wall and photographs of test section showing condensation. 0.418 in. (1.062 cm) inside-diameter steam nozzle; $V_{i,l} = 30$ ft/sec (9.1 m/s); $V_{i,v} = 1100$ ft/sec (335 m/s); $p_{i,v} = 15$ lbf/in^2 (103 kN/m^2).

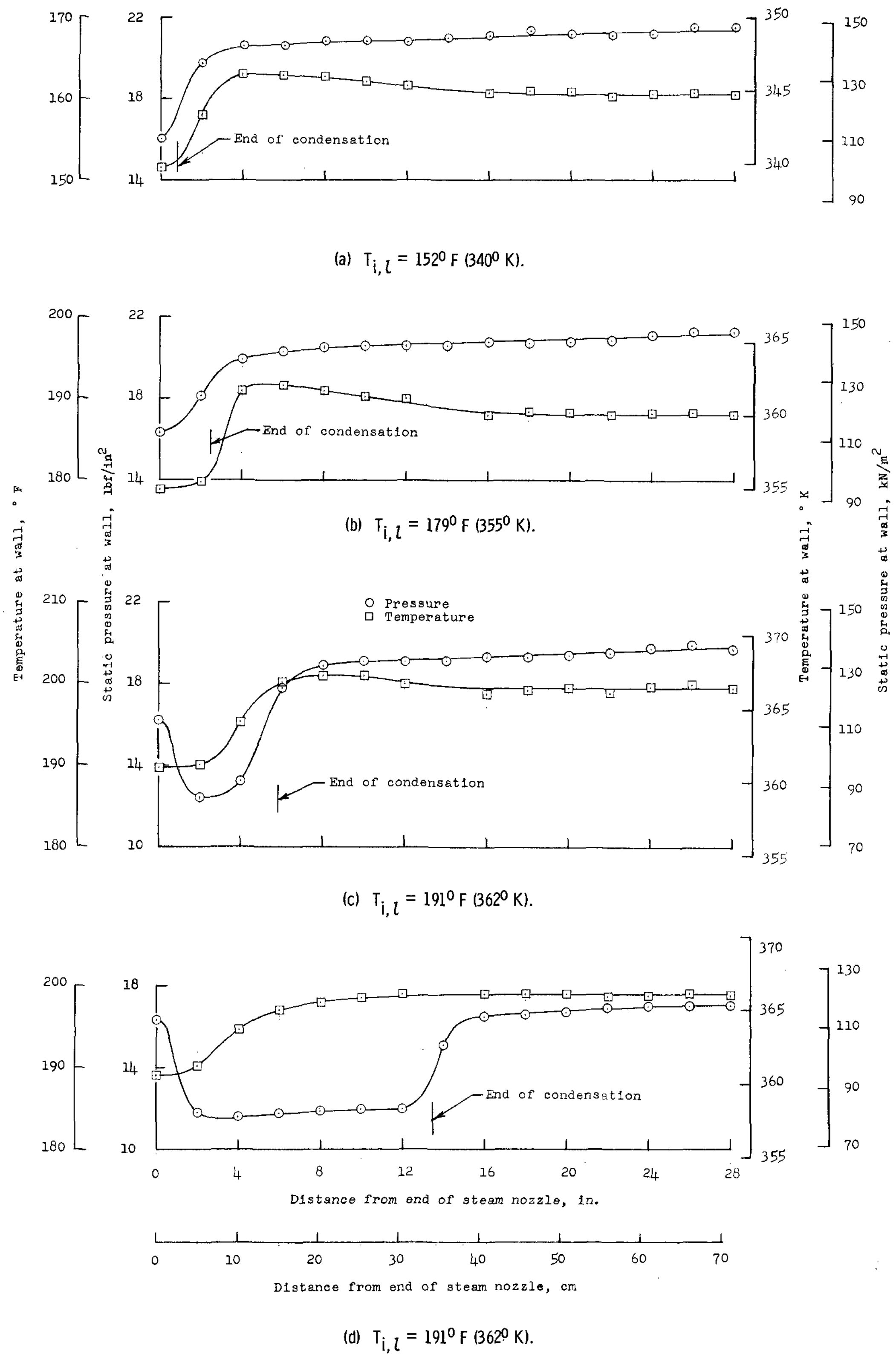

Figure 5.- Typical temperature and pressure distributions along test-section wall. 0.316 in. (0.803 cm) inside-diameter steam nozzle; $V_{i,l}$ = 30 ft/sec (9.1 m/s); $V_{i,v}$ = 1100 ft/sec (335 m/s); $p_{i,v}$ = 15 lbf/in² (103 kN/m²).

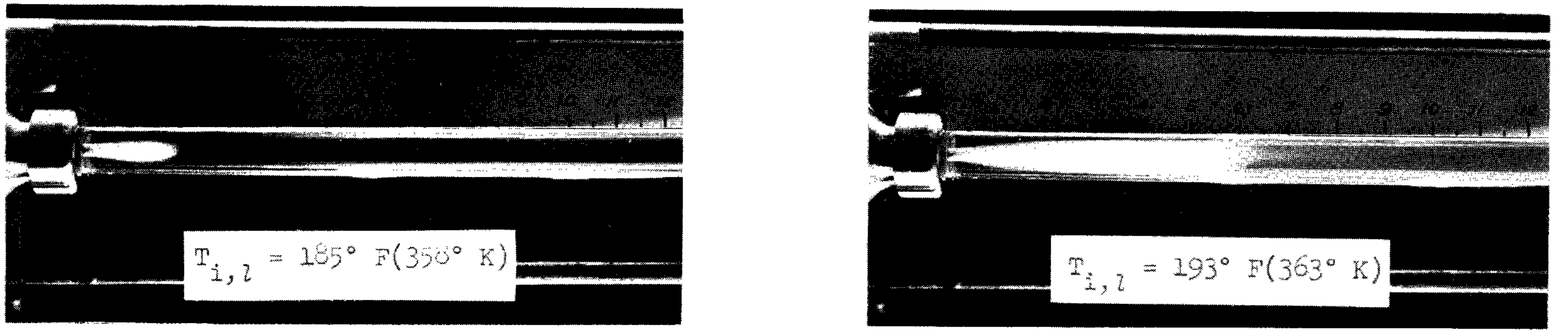

(a) 0.158 in. (0.401 cm) inside-diameter steam nozzle.

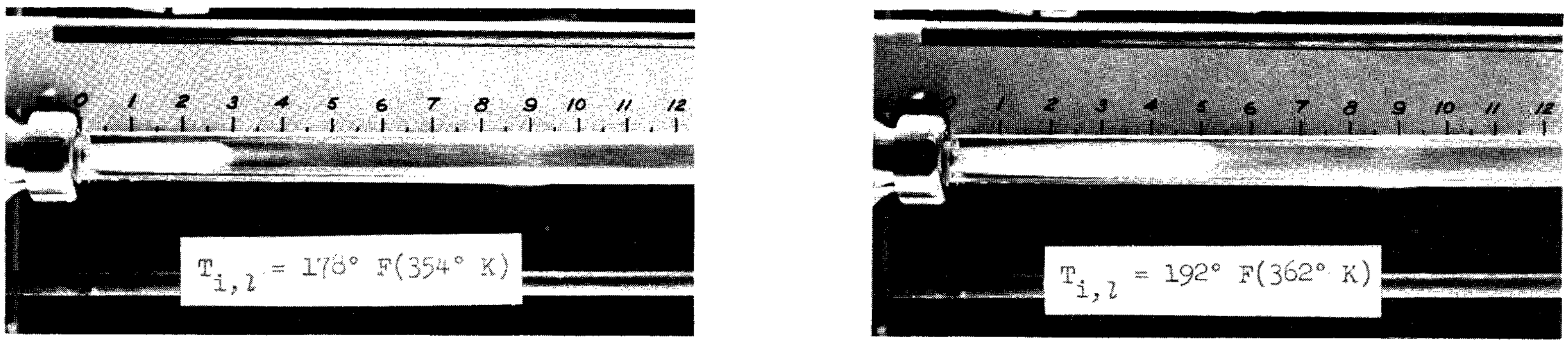

(b) 0.316 in. (0.803 cm) inside-diameter steam nozzle.

L-65-143

Figure 6.- Typical condensation photographs of two steam nozzles. $V_{i,l}$ = 30 ft/sec (9.1 m/s); $V_{i,v}$ = 800 ft/sec (244 m/s); $p_{i,v}$ = 15 lbf/in^2 (103 kN/m^2).

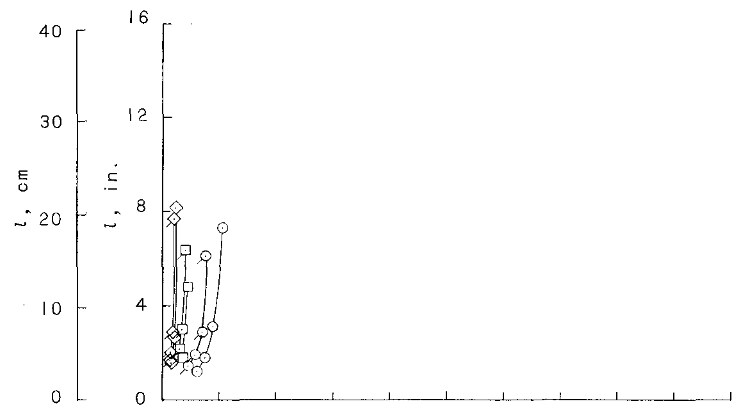

(a) 0.158 in. (0.401 cm) inside-diameter nozzle; $p_{i,v}$ = 15 lbf/in^2 (103 kN/m^2).

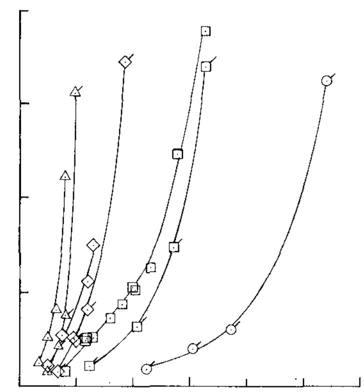

(b) 0.316 in. (0.803 cm) inside-diameter nozzle; $p_{i,v}$ = 15 lbf/in^2 (103 kN/m^2).

$V_{i,l}$, ft/sec	(m/s)	$V_{i,v}$, ft/sec (m/s): 600 (183)	800 (244)	1100 (335)
20	(6.1)	○	○	○
30	(9.1)	□	□	□
45	(13.7)	◇	◇	◇
60	(18.3)	△	△	△

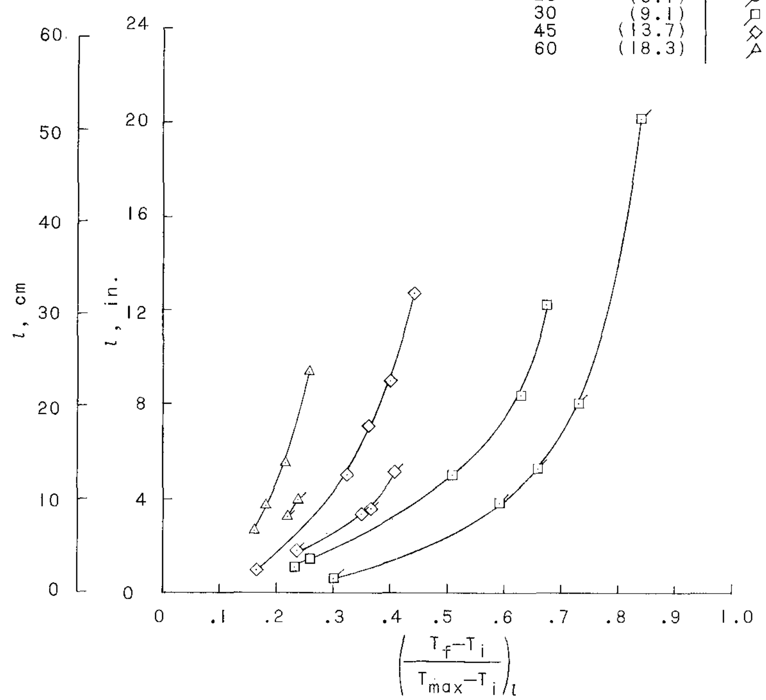

(c) 0.418 in. (1.062 cm) inside-diameter nozzle; $p_{i,v}$ = 15 lbf/in^2 (103 kN/m^2).

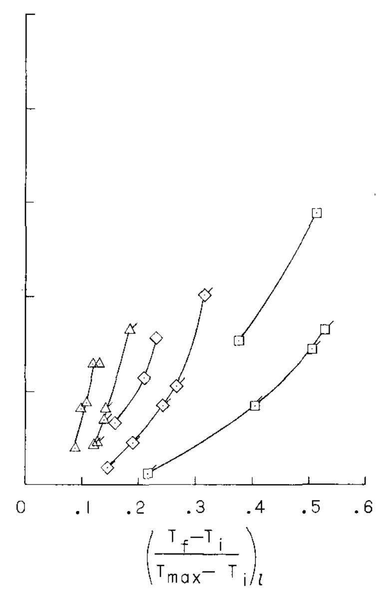

(d) 0.418 in. (1.062 cm) inside-diameter nozzle; $p_{i,v}$ = 10 lbf/in^2 (69 kN/m^2).

Figure 7.- Variation of condensation length with temperature-rise parameter.

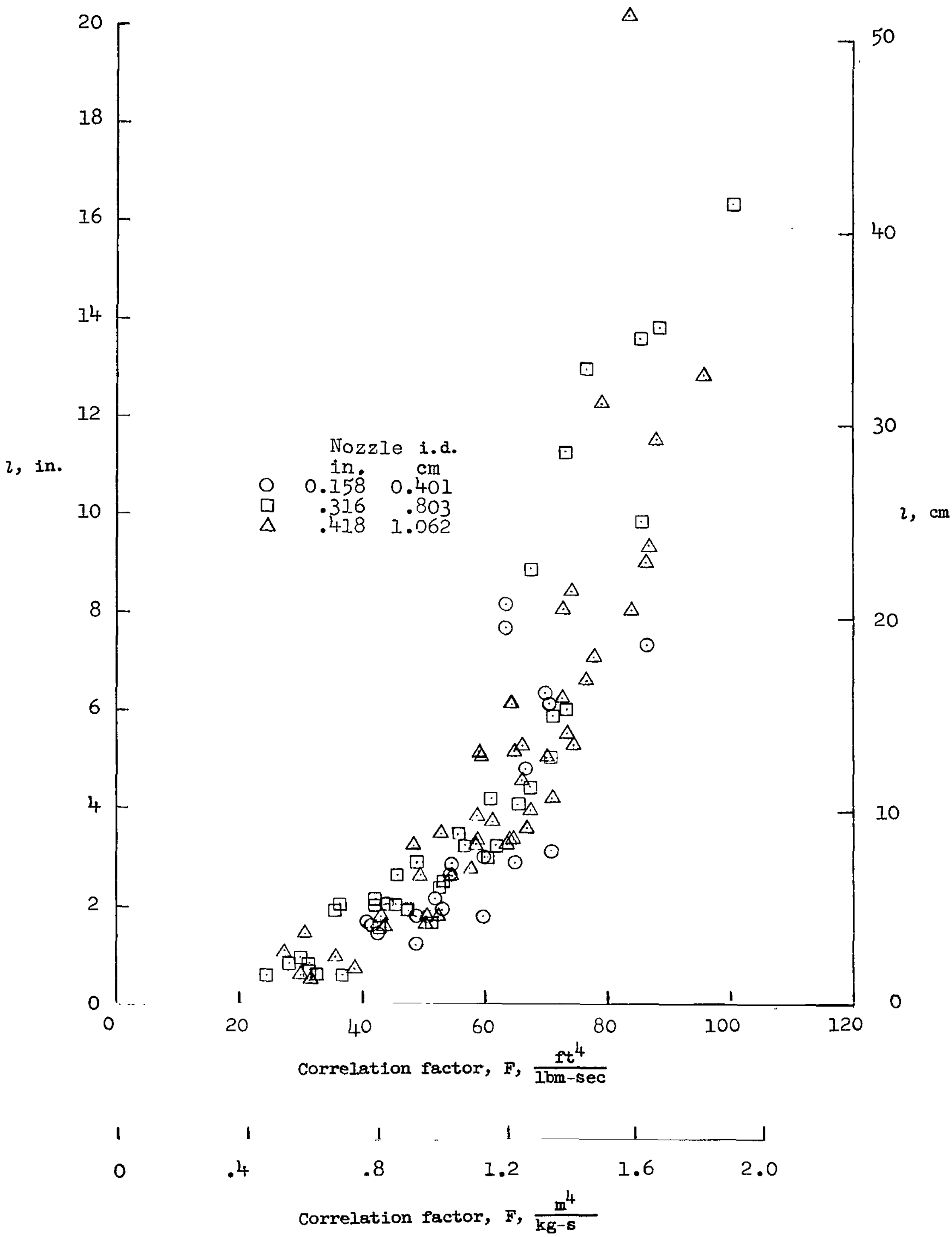

Figure 8.- Variation of condensation length with correlation factor.

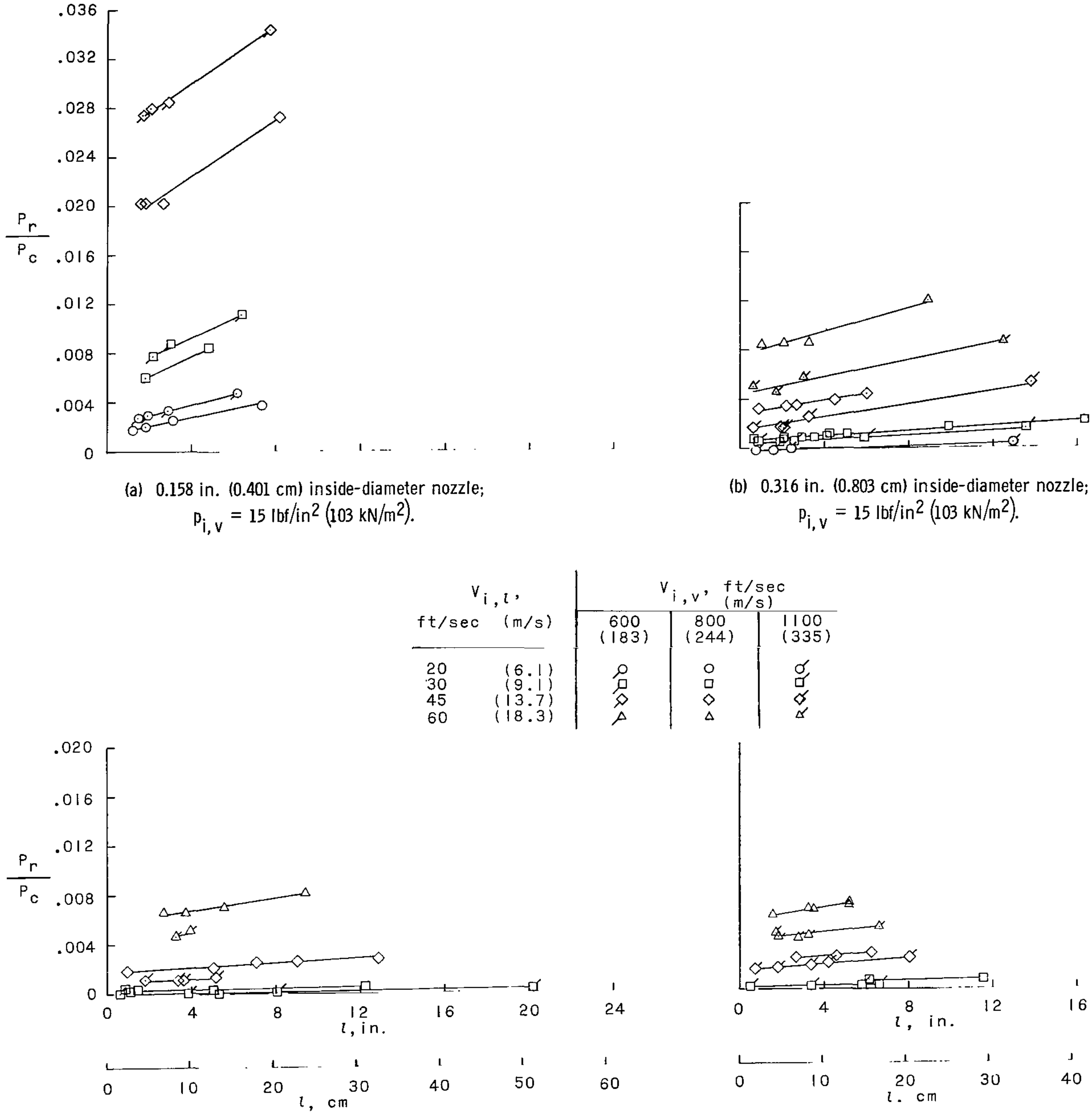

(a) 0.158 in. (0.401 cm) inside-diameter nozzle; $p_{i,v} = 15\ \text{lbf/in}^2\ (103\ \text{kN/m}^2)$.

(b) 0.316 in. (0.803 cm) inside-diameter nozzle; $p_{i,v} = 15\ \text{lbf/in}^2\ (103\ \text{kN/m}^2)$.

(c) 0.418 in. (1.062 cm) inside-diameter nozzle; $p_{i,v} = 15\ \text{lbf/in}^2\ (103\ \text{kN/m}^2)$.

(d) 0.418 in. (1.062 cm) inside-diameter nozzle; $p_{i,v} = 10\ \text{lbf/in}^2\ (69\ \text{kN/m}^2)$.

Figure 9.- Variation with condensation length of the ratio of pumping power required to the power equivalent of the heat transferred in the condensation process.

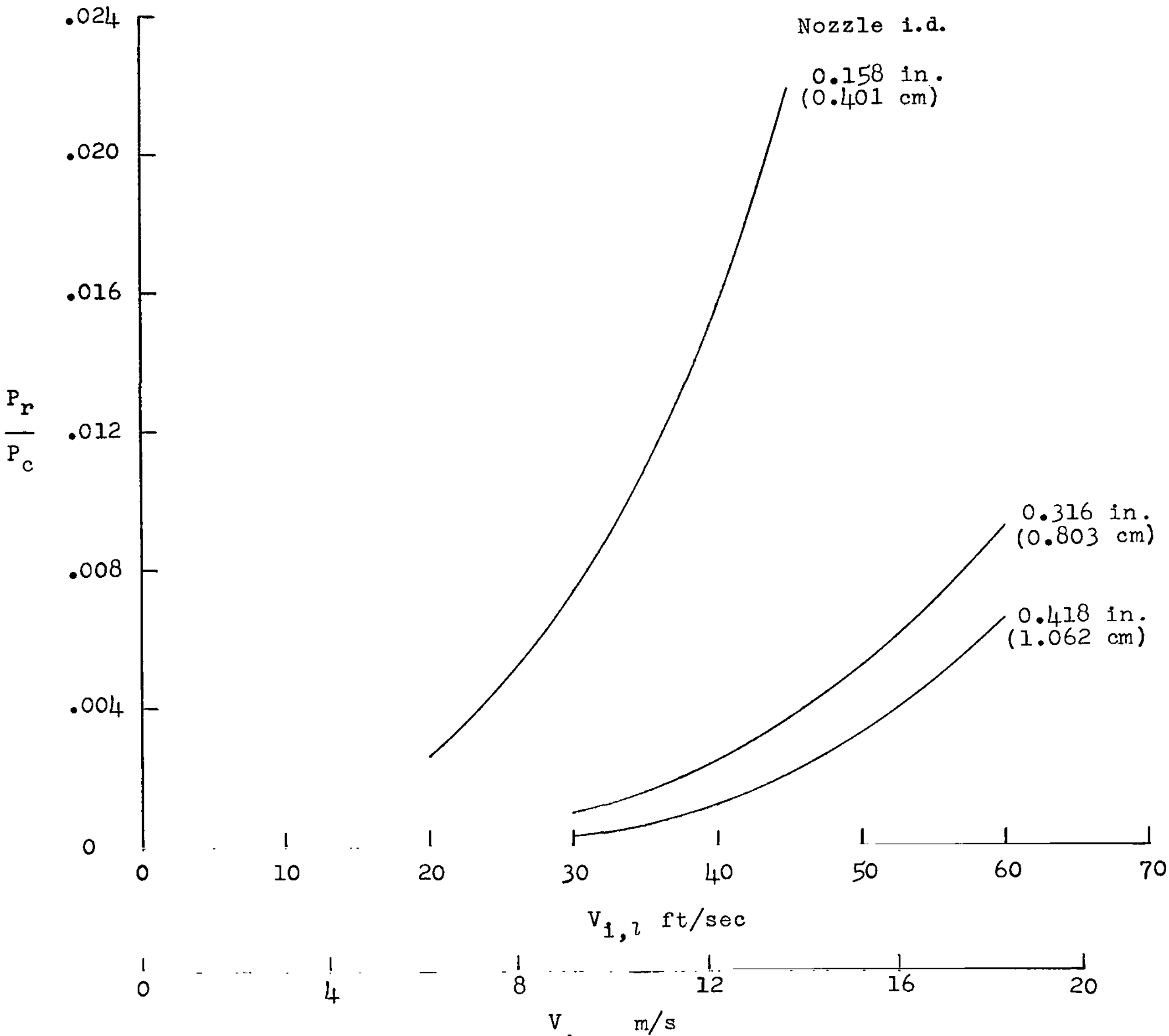

Figure 10.- Variation with initial water velocity of the ratio of pumping power required to the power equivalent of the heat transferred in the condensation process. $V_{i,v}$ = 800 ft/sec (244 m/s); $p_{i,v}$ = 15 lbf/in^2 (103 kN/m^2); l = 3.6 in. (9.1 cm).

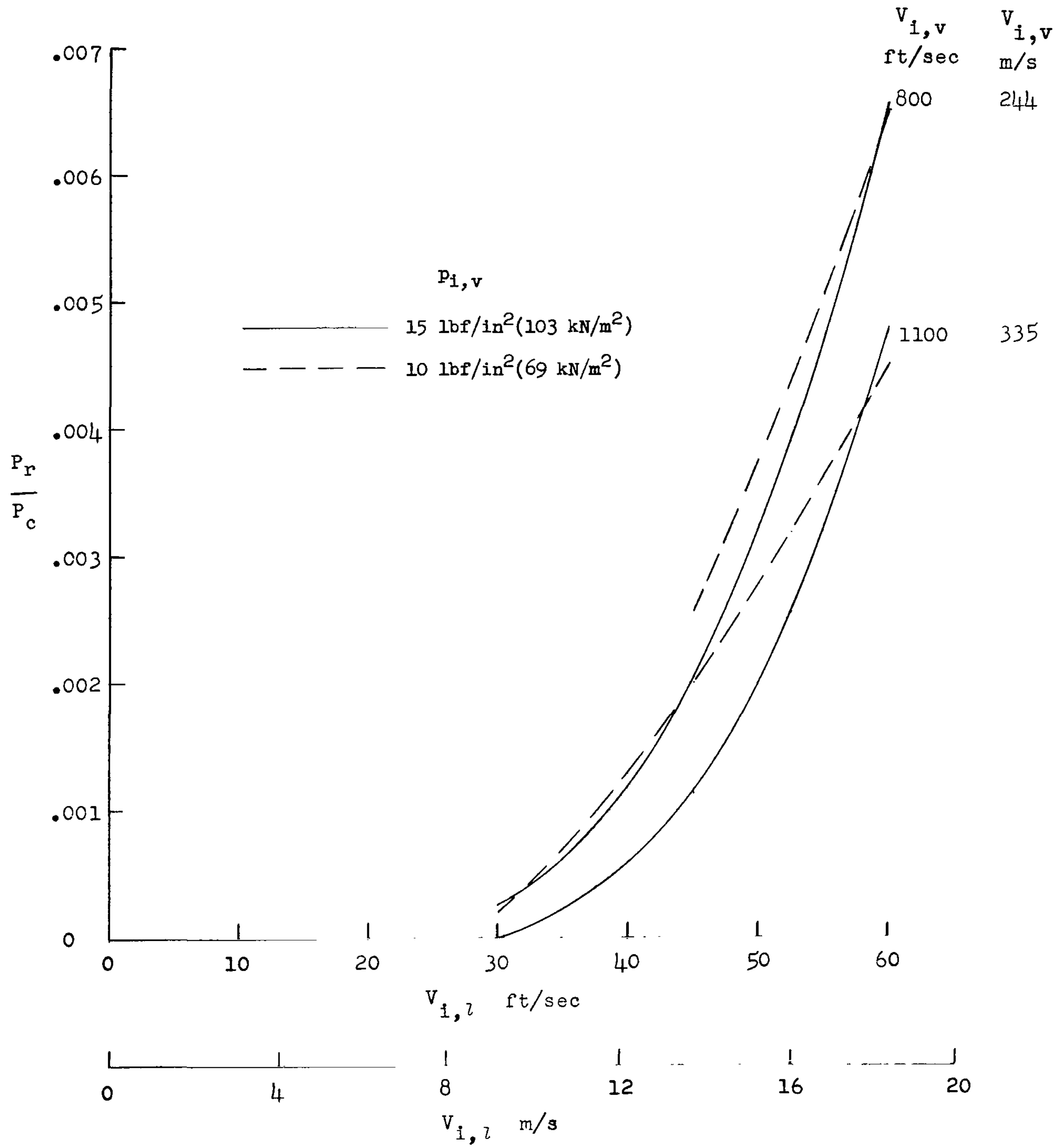

Figure 11.- Effect of steam static pressure on the ratio of pumping power required to the power equivalent of the heat transferred in the condensation process. 0.418 in. (1.062 cm) inside-diameter steam nozzle; l = 3.6 in. (9.1 cm).

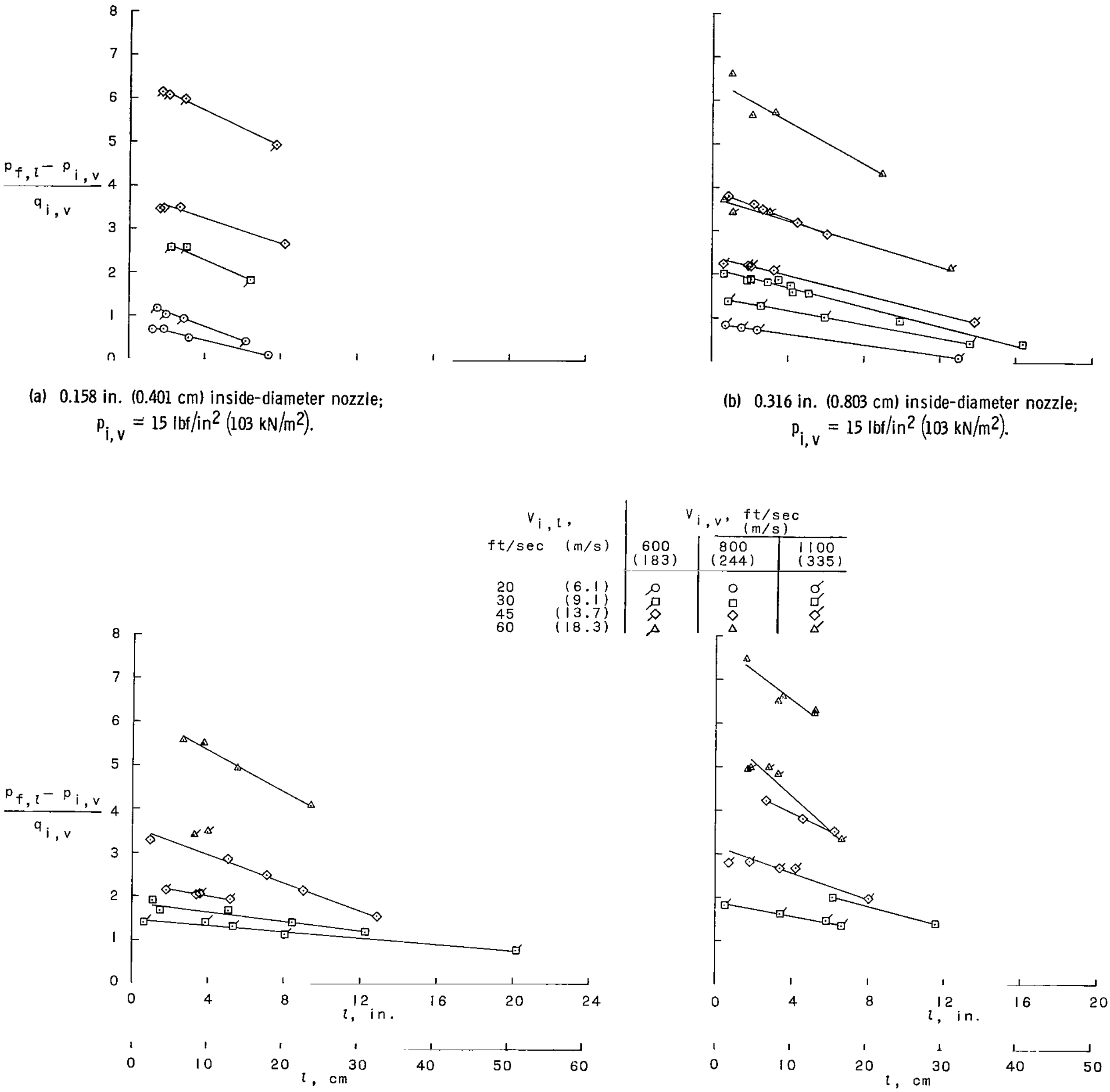

(a) 0.158 in. (0.401 cm) inside-diameter nozzle; $p_{i,v}$ = 15 lbf/in^2 (103 kN/m^2).

(b) 0.316 in. (0.803 cm) inside-diameter nozzle; $p_{i,v}$ = 15 lbf/in^2 (103 kN/m^2).

(c) 0.418 in. (1.062 cm) inside-diameter nozzle; $p_{i,v}$ = 15 lbf/in^2 (103 kN/m^2).

(d) 0.418 in. (1.062 cm) inside-diameter nozzle; $p_{i,v}$ = 10 lbf/in^2 (69 kN/m^2).

Figure 12.- Variation of condensate static-pressure-rise coefficient with condensation length.

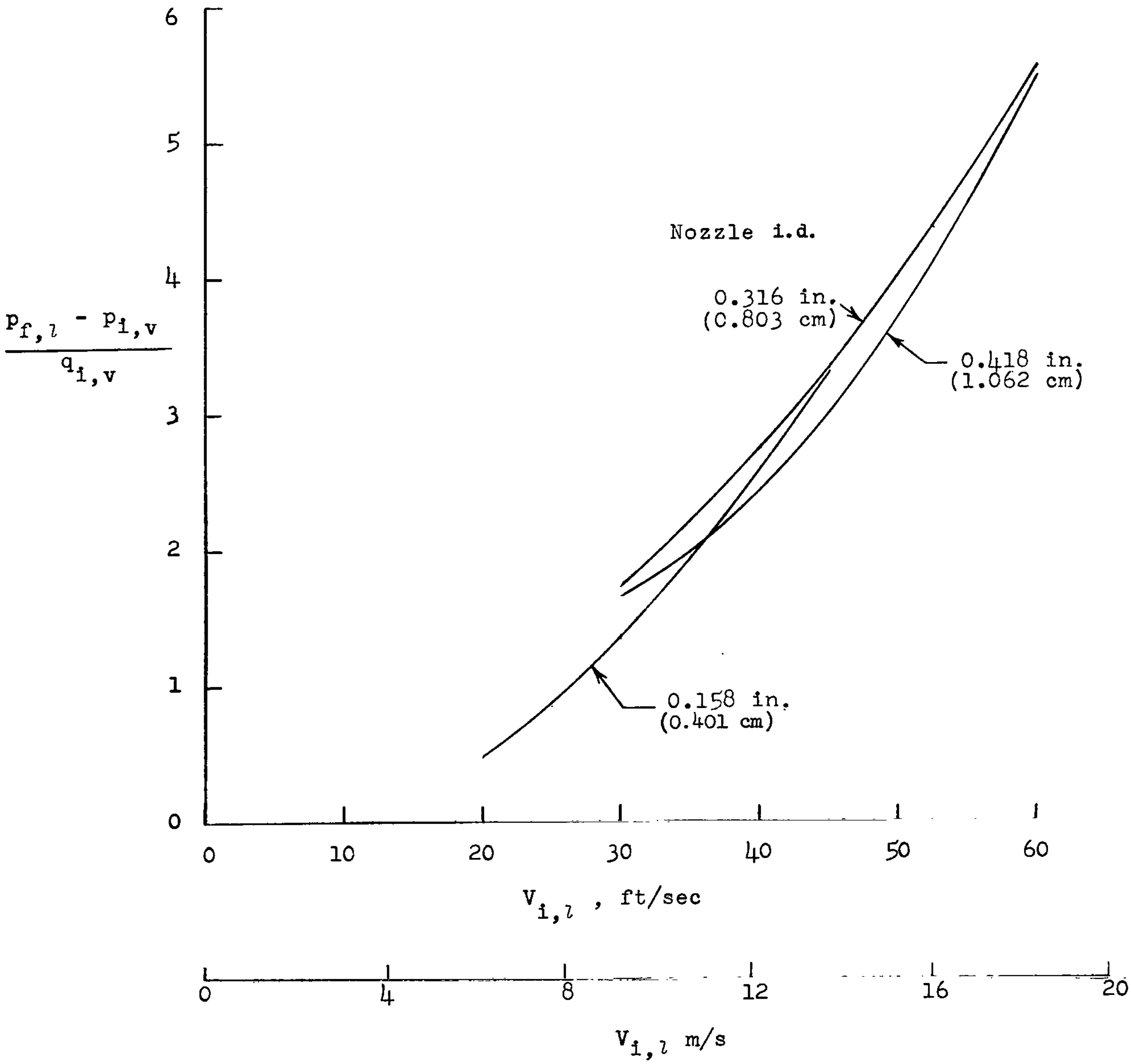

Figure 13.- Variation of condensate static-pressure-rise coefficient with initial water velocity. $V_{i,v}$ = 800 ft/sec (244 m/s); $p_{i,v}$ = 15 lbf/in^2 (103 kN/m^2); l = 3.6 in. (9.1 cm).

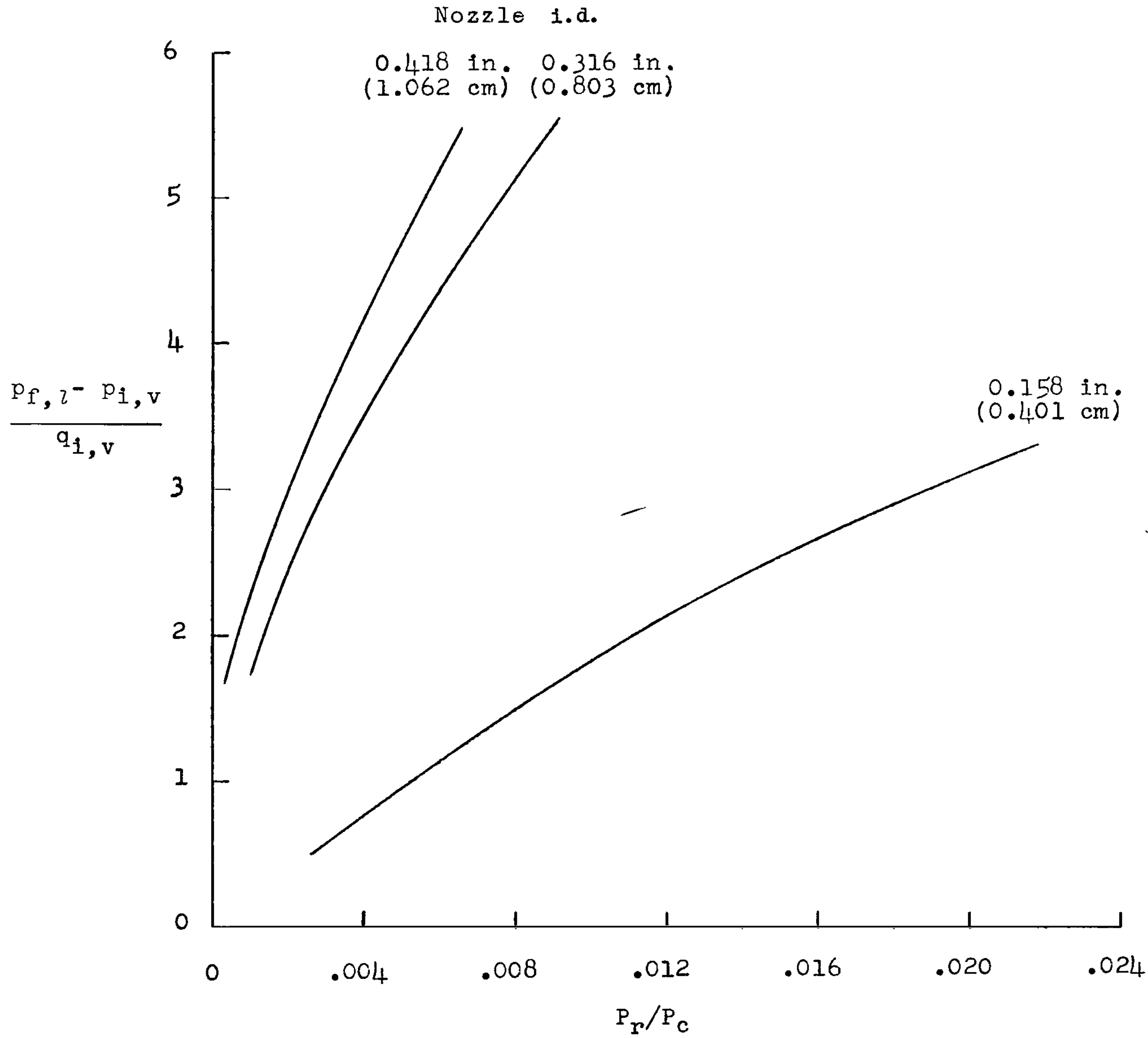

Figure 14.- Variation of condensate static-pressure-rise coefficient with pumping power-required ratio. $V_{i,v}$ = 800 ft/sec (244 m/s); $p_{i,v}$ = 15 lbf/in^2 (103 kN/m^2); l = 3.6 in. (9.1 cm).

3) 1 8 1 8 0 8

"The aeronautical and space activities of the United States shall be conducted so as to contribute . . . to the expansion of human knowledge of phenomena in the atmosphere and space. The Administration shall provide for the widest practicable and appropriate dissemination of information concerning its activities and the results thereof."

—NATIONAL AERONAUTICS AND SPACE ACT OF 1958

NASA SCIENTIFIC AND TECHNICAL PUBLICATIONS

TECHNICAL REPORTS: Scientific and technical information considered important, complete, and a lasting contribution to existing knowledge.

TECHNICAL NOTES: Information less broad in scope but nevertheless of importance as a contribution to existing knowledge.

TECHNICAL MEMORANDUMS: Information receiving limited distribution because of preliminary data, security classification, or other reasons.

CONTRACTOR REPORTS: Technical information generated in connection with a NASA contract or grant and released under NASA auspices.

TECHNICAL TRANSLATIONS: Information published in a foreign language considered to merit NASA distribution in English.

TECHNICAL REPRINTS: Information derived from NASA activities and initially published in the form of journal articles.

SPECIAL PUBLICATIONS: Information derived from or of value to NASA activities but not necessarily reporting the results of individual NASA-programmed scientific efforts. Publications include conference proceedings, monographs, data compilations, handbooks, sourcebooks, and special bibliographies.

Details on the availability of these publications may be obtained from:

SCIENTIFIC AND TECHNICAL INFORMATION DIVISION

NATIONAL AERONAUTICS AND SPACE ADMINISTRATION

Washington, D.C. 20546